



## OPEN Time derivatives of weak values

Xavier Oriols

The time derivative of a physical property often gives rise to another meaningful property. Since weak values provide empirical insights that cannot be derived from expectation values, this paper explores what physical properties can be obtained from the time derivative of weak values. It demonstrates that, in general, the time derivative of a weak value that is invariant under an electromagnetic gauge transformation is neither a weak value nor a gauge-invariant quantity. Left- and right-hand time derivatives of a weak value are defined, and two necessary and sufficient conditions are presented to ensure that they are also gauge-invariant weak values. Finite-difference approximations of the left- and right-hand time derivatives of weak values are also presented, yielding results that match the theoretical expressions when these are gauge invariant. With these definitions, a local Ehrenfest-like theorem can be derived, giving a natural interpretation for the time derivative of weak values. Notably, a single measured weak value of the system's position provides information about two additional unmeasured weak values: the system's local velocity and acceleration, through the first- and second-order time derivatives of the initial weak value, respectively. These findings also offer guidelines for experimentalists to translate the weak value theory into practical laboratory setups, paving the way for innovative quantum technologies. An example illustrates how the electromagnetic field can be determined at specific positions and times from the first- and second-order time derivatives of a weak value of position.

**Keywords** Weak values, Time derivative, Gauge invariance, Quantum electromagnetic sensors

### Abbreviations

POVM	Positive-operator-valued measure
PVM	Projection-valued measure
LHD	Left-hand derivative
RHD	Right-hand derivative
FDLHD	Finite-difference left-hand derivative
FDRHD	Finite-difference right-hand derivative

The primary goal of science is to construct models that successfully predict empirical results. Weak values are an original way of predicting novel properties of quantum systems<sup>1–23</sup> which are empirically observable in the laboratory<sup>24–45</sup>. This new information offered by weak values cannot be accessed through expectation values. In physics, the time derivative of a physical property often leads to another meaningful property. It remains an open question whether this relationship holds for the time derivatives of weak values. This paper investigates such a relationship.

Weak values are generating increasing interest in the scientific community. They have been employed to explore novel properties such as the position-dependent velocity of particles in either non-relativistic<sup>5,6</sup> or relativistic<sup>7</sup> scenarios, thermalized kinetic energies<sup>8,9</sup> as well as tunneling and arrival times<sup>10–13</sup>. Weak values have been invoked in cosmological contexts, such as inflation theory<sup>14</sup> and the back-reaction of the Hawking radiation from black holes<sup>17</sup>. In quantum information science, they have been applied to quantum computation<sup>18</sup>, quantum communication<sup>19</sup>, and quantum sensing<sup>20</sup>.

There are many experimental protocols for weak values in optical and solid-state platforms<sup>24–32</sup>. Relevant experiments conducted with weak values include the three-box paradox<sup>39</sup>, the violation of the Leggett-Garg inequality<sup>40</sup>, the detection of the superluminal signals<sup>41</sup> and the measurement of Bohmian trajectories<sup>42</sup>. Since weak values are expressed as quotients, a small denominator (i.e., quasi-orthogonal pre- and post-selected states) can be used to amplify the spin Hall effect of light<sup>43</sup>, optimize the signal-to-noise ratio<sup>44</sup> and measure small changes in optical frequencies<sup>45</sup>.

This paper aims to explore the additional physical insights that can be gained about the behavior of quantum systems by analyzing not only weak values, but also their time derivatives. Wiseman was the first to discuss the time derivative of weak values<sup>5</sup>, presenting a local velocity derived from the time derivative of a weak value of

Universitat Autònoma de Barcelona, 08193 Bellaterra, Spain. email: xavier.oriols@uab.es

the position<sup>1</sup>. This paper examines the time derivatives of weak values from a general perspective using arbitrary operators. In general, the time derivative of a weak value reveals a much richer phenomenology than the time derivatives of expectation values. In many cases, the time derivative of a weak value is neither a weak value nor invariant under an electromagnetic gauge transformation.

A quantity that is not invariant under an electromagnetic gauge transformation cannot be measured in a laboratory. The electromagnetic vector and scalar potentials are the typical examples of the utility and unmeasurability of gauge-dependent elements<sup>47–51</sup> (with the Aharonov-Bohm effect being its most iconic example<sup>52</sup>). Similarly, a weak value or its time derivatives are empirically observable in the laboratory only when they are gauge invariant. Several examples of observable and unobservable weak values and their time derivative will be discussed in the paper. For example, it is known that the wave function depends on the electromagnetic gauge<sup>52–54</sup>. Thus, strictly speaking, the wave function cannot be empirically measured through a weak value.

The ontological meaning of weak values remains controversial, ranging from being mere mathematical transition amplitudes in most orthodox views<sup>55,56</sup>, to representing basic elements in alternative interpretations of quantum phenomena<sup>4,57–61</sup>. For example, the meaning of weak values has been interpreted in the context of the two-state vector formalism of quantum mechanics<sup>1–4</sup>, consistent histories<sup>21</sup>, and Bohmian or modal interpretations<sup>22,23</sup>. Controversies surrounding weak values also arise in debates about which empirical procedures can reliably measure a weak value in the laboratory. It is argued that weak values are measured from conditional probabilities obtained from a large ensemble of identically prepared systems<sup>62</sup>. In a recent experiment, however, a weak value was measured “with just a single click,” without requiring statistical averaging<sup>63</sup>. It has also been argued that weak values can, in fact, be measured using strong measurements<sup>64</sup>. The widely accepted consensus around the concept of weak values is the mathematical expression that defines a weak value. This mathematical expression, which is sufficient for all developments and conclusions in this paper, can be derived from all common quantum theories regardless of the ontological meaning attributed to weak values, and the resulting predictions can subsequently be tested in the laboratory, irrespective of the specific experimental protocol used. Thus, weak values (and their time derivatives) possess predictive power and offer novel ways to characterize quantum systems without the need to select a particular ontological interpretation or a fixed measurement protocol. Therefore, all results presented in this paper are ontologically neutral (valid under any interpretation of quantum mechanics). Similarly, we do not need to specify any ontological status for gauge-dependent elements to draw the conclusions of this paper<sup>2</sup>.

The structure of the remainder of the paper is as follows. In the rest of this introduction, we revisit the role of electromagnetic gauge invariance in non-relativistic quantum mechanics, particularly regarding expectation values and their time derivatives. In Section “[Time derivative of weak values](#)”, we present the time derivatives of weak values and the conditions under which they are gauge invariant. In Section “[Finite-difference approximations](#)”, we present finite-difference approximations of the left- and right-hand time derivatives of weak values, and we show that they yield results identical to the theoretical ones when the latter are gauge invariant. In Section “[Examples on Gauge invariance of weak values](#)”, we explore how gauge invariance determines the empirical observability of typical weak values. Section “[Examples on the time derivative of weak values](#)” introduces several examples of time derivatives of weak values like the local velocity, the local version of the work-energy theorem, and the local Lorentz force, leading to local quantum sensors of the electromagnetic field. In Section “[Which modal theories exhibit time-dependent consistency of weak values?](#)”, we discuss which pre- and post-selected states provide time derivatives of weak values consistent with the time derivative of expectation values. Finally, Section “[Conclusions](#)” explains the main conclusion. Several Online Appendices detail the discussions presented in the paper.

## Gauge invariance in quantum mechanics

Although they can also be formulated for many-particle scenarios<sup>8,9</sup>, weak values become especially relevant when discussing the properties of a single particle. All the results in the present paper are developed within the so-called semi-classical approach to light–matter interaction, in the sense that the electron (i.e., matter) is treated as a quantum particle, while the electromagnetic fields or potentials (i.e., light) are treated as classical fields,

<sup>1</sup>The word *local* in this paper is defined in contrast to *global*. The expectation value of the velocity represents a *global* quantity, as it does not account for how velocity is distributed across different positions, while the weak value of the velocity, when post-selected at a given position, provides a *local* velocity at that position. In a two-particle system, the term local could be ambiguous because a *local* velocity at a point in configuration space may correspond to two *non-local* velocities in physical space Ref.46. In any case, for the single-particle systems considered in this work, the term *local* will be unproblematic.

<sup>2</sup>The concept of a “true physical quantity” is defined in Ref.52 as: “a quantity whose value at any time does not depend (for a given motion of the system) on the gauge used to describe the electromagnetic field.” This definition suggests ontological consequences, as other gauge-dependent properties are referred to as “non-physical quantities.” However, as mentioned in the introduction, such ontological implications are not necessary for discussing the results in this paper Refs.65,66. The analogy between electromagnetic potentials and angles, both exhibiting *redundancies*, clarifies this point. The direction of a physical system specified by an angle  $\theta$  or by another  $\theta + 2\pi n$ , with  $n \in \mathbb{Z}$ , is the same. Thus, the angle specifying the direction of a physical system cannot be directly measured as a unique number, because there are infinite equivalent angles corresponding to the same physical system. However, this *redundancy* of the angle does not directly imply that  $\theta$  is an “unphysical” parameter. Similarly, the discussion of how the *redundancy* of electromagnetic potentials affects their direct measurability is indeed pertinent here. However, the question of how this *redundancy* affects the “physicality” of the electromagnetic potentials is a different and much more subtle debate.

affecting the electron as external potentials, but without being affected themselves by the electron<sup>3</sup>. In particular, we will deal with a non-relativistic spinless particle of mass  $m^*$  interacting with a classical electromagnetic field.

The Hamiltonian of the system, in the Coulomb gauge, is written as<sup>52–54</sup>

$$H = H(\mathcal{A}, A) = \frac{1}{2m^*} (\hat{P} - q\mathcal{A})^2 + qA, \quad (1)$$

where  $q$  is the charge of the particle,  $\hat{P} = -i\hbar\nabla$  is the canonical momentum operator, and  $A$  and  $\mathcal{A}$  are the scalar and vector electromagnetic potentials, respectively. The evolution of the wave function  $\psi(x, t) = \langle x|\psi(t)\rangle$  is given by the Schrödinger equation

$$i\hbar \frac{\partial \psi(x, t)}{\partial t} = H(\mathcal{A}, A)\psi(x, t). \quad (2)$$

It is well-known that a different set of potentials (indicated by the superscript  $g$ ) given by<sup>52–54</sup>

$$\mathcal{A}^g = \mathcal{A} + \nabla g \quad \text{and} \quad A^g = A - \frac{\partial g}{\partial t}, \quad (3)$$

keeps the overall theory invariant in the sense that the observable properties remain the same in any gauge. Here,  $g = g(x, t)$  is any sufficiently regular real function (apart from having space and time derivatives,  $g(x, t)$  must be single-valued.) over  $3D$  space plus time  $t$ . For example, the electric and magnetic fields are gauge invariant and defined as  $E = -\nabla A^g - \frac{\partial \mathcal{A}^g}{\partial t}$  and  $B = \nabla \times \mathcal{A}^g$ , respectively. In this paper, according to the above notation in Eq. (3), any symbol (for a state, eigenvalue, operator, etc.) without a superscript  $g$  should be interpreted either as a gauge-invariant element or as an element defined within the Coulomb gauge.

When using a general gauge, to keep the same structure of the Schrödinger equation in (2), a gauge-dependent Hamiltonian  $H^g$  and a gauge-dependent wave function  $\psi^g(x, t)$  are needed<sup>52–54</sup>. See Online Appendix A for details and Ref.<sup>52–54</sup>. The new-gauge Hamiltonian  $H^g$  is given by

$$H^g := H(\mathcal{A}^g, A^g) = e^{i\frac{q}{\hbar}g} \left( H(\mathcal{A}, A) - q\frac{\partial g}{\partial t} \right) e^{-i\frac{q}{\hbar}g}, \quad (4)$$

and the new-gauge wave function  $\psi^g(x, t)$  is given by:

$$\langle x|\psi^g(t)\rangle = \langle x|\hat{G}(t)|\psi\rangle = \psi^g(x, t) = e^{i\frac{q}{\hbar}g(x,t)}\psi(x, t), \quad (5)$$

where  $\hat{G}(t)$  is a local operator whose position representation is  $\langle x|\hat{G}(t)|x'\rangle = \langle x|e^{i\frac{q}{\hbar}g}|x'\rangle = e^{i\frac{q}{\hbar}g(x,t)}\delta(x - x')$ . This arbitrary gauge allows an infinite set of possible Hamiltonians, electromagnetic potentials, and wave functions<sup>47–50</sup>.

Finally, depending on the gauge, the wave function evolution can be equivalently written in terms of the (Coulomb gauge) time-evolution operator as  $|\psi(t_R)\rangle = \hat{U}(t_R)|\psi(0)\rangle$  or in a general gauge as  $|\psi^g(t_R)\rangle = \hat{U}^g(t_R)|\psi^g(0)\rangle$ . As shown in Online Appendix B (see also<sup>67</sup>), the gauge dependence of the time evolution operator  $\hat{U}(t)$  is

$$\hat{U}^g(t) := \hat{G}(t)\hat{U}(t)\hat{G}^\dagger(0) = \hat{\mathbb{T}}e^{-\frac{i}{\hbar}\int_0^t \hat{H}(\mathcal{A}^g, A^g)dt'}, \quad (6)$$

in agreement with the gauge-dependent Hamiltonian in Eq. (4) with  $\hat{\mathbb{T}}$  being the time-ordering integral operator and  $\hat{G}^\dagger(t)$  defined such that  $\hat{G}(t)\hat{G}^\dagger(t) = \mathbb{1}$ .

### Time derivative of expectation values

The time derivative of weak values shows similarities and differences with the time derivative of expectation values. In this subsection, a brief explanation of the expectation values and their time derivatives is presented.

We consider an ensemble of identical quantum states  $|\psi\rangle = |\psi(0)\rangle$  prepared at the initial time  $t = 0$ . Such an initial state evolves until time  $t$  when a measurement of an output linked to the operator  $\hat{O}$  is made. The relationship between the measured output and the hermitian operator  $\hat{O}$  is determined through a positive-operator-valued measure (POVM) or a projection-valued measure (PVM)<sup>68,69</sup>. The expectation value  $\mathcal{E}$  is given by

$$\mathcal{E}(\hat{O}, t|\psi) := \langle \psi|\hat{U}^\dagger(t)\hat{O}\hat{U}(t)|\psi\rangle = \langle \psi(t)|\hat{O}|\psi(t)\rangle, \quad (7)$$

<sup>3</sup>If the electromagnetic fields are treated quantum mechanically, allowing the self-consistent exchange of energy between light and matter, the problem of gauge invariance remains. A simple way to see this is through the so-called canonical quantization of the electromagnetic field—an approach sometimes criticized for being too heuristic but widely used in textbooks. The quantum Hamiltonian of light and matter is obtained from the semi-classical Hamiltonian in Eq. (1) by promoting the classical fields to field operators. However, other equally valid (gauge-dependent) quantum Hamiltonians can be obtained using the same canonical quantization procedure when starting from different (gauge-dependent) semi-classical Hamiltonians in Eq. (4).

The notation of the left-hand side of Eq. (7) indicates that the expectation value is evaluated for the operator  $\hat{O}$  and conditioned on  $|\psi\rangle$  (i.e., the same property gives a different expectation value if the quantum state changes).

As reported in the literature<sup>48,52</sup>, the condition for  $\mathcal{E}(\hat{O}, t_R|\psi)$  to be empirically observable (i.e., gauge invariant) is that the same value has to be obtained in the laboratory for the Coulomb or any other gauge,  $\langle\psi(t)|\hat{O}|\psi(t)\rangle = \langle\psi^g(t)|\hat{O}^g|\psi^g(t)\rangle$ . Using Eqs. (5) and (6), the necessary and sufficient condition on the operator  $\hat{O}$  for the empirical observability of  $\mathcal{E}(\hat{O}, t|\psi)$  for any state  $|\psi\rangle$  is then,

$$\text{C1: } \hat{O}^g := \hat{O}(\hat{\mathcal{A}}^g, \hat{A}^g) = \hat{G}\hat{O}(\hat{\mathcal{A}}, \hat{A})\hat{G}^\dagger.$$

When this condition is satisfied, one gets the same expectation value in any gauge.

The preparation (pre-selection) of the initial state  $|\psi\rangle$  used in Eq. (7) to evaluate an expectation value is not free of gauge ambiguities. The Hilbert space representation of the quantum state is a gauge-dependent object, as shown in Eq. (5). Thus, the preparation of the initial state  $|\psi^g\rangle$  is achieved by detecting a measurable property  $\lambda^g$  of the system (not the initial quantum state itself). Let us define  $\hat{\Lambda}^g$  as the operator used to detect such a property as follows  $\hat{\Lambda}^g|\psi^g\rangle = \lambda^g|\psi^g\rangle$ . We discuss below the condition on  $\hat{\Lambda}^g$  to ensure that  $\lambda^g = \lambda$  is gauge invariant (i.e., empirically measurable). Using  $|\psi^g\rangle = \hat{G}|\psi\rangle$  as in Eq. (5), the previous eigenvalue equation in an arbitrary gauge  $\hat{\Lambda}^g|\psi^g\rangle = \lambda^g|\psi^g\rangle$  can be written as  $\hat{\Lambda}^g\hat{G}|\psi\rangle = \lambda^g\hat{G}|\psi\rangle$ . Thus, to have  $\lambda^g = \lambda$ , the necessary and sufficient condition on the operator  $\hat{\Lambda}$  is

$$\text{C2: } \hat{\Lambda}^g := \hat{\Lambda}(\hat{\mathcal{A}}^g, \hat{A}^g) = \hat{G}\hat{\Lambda}(\hat{\mathcal{A}}, \hat{A})\hat{G}^\dagger,$$

In agreement with Eq. (5), when C2 is satisfied, the direct measurement of the initial state  $|\psi^g\rangle$  is not accessible, but one can infer that the quantum system is  $|\psi^g\rangle$  (in any gauge) by the measurement of the (gauge invariant) eigenvalue  $\lambda$ . In summary, condition C2 shows that, if Eq. (7) wants to be measured in the laboratory, the initial state  $|\psi\rangle$  has to be empirically identified in the laboratory through the measurement of the gauge invariant value  $\lambda$ .

A list of common operators and their accomplishment or not of C1 and C2 is presented in Table 1.<sup>4</sup>

Writing explicitly its  $t$ -dependence in Eq. (7) allows us to describe the time derivative of expectation values. From  $\mathcal{E}(\hat{O}, t|\psi)$ , using

$$\frac{\partial \hat{U}(t)}{\partial t} = -\frac{i}{\hbar} \hat{H}(t)\hat{U}(t) \tag{8}$$

and its complex conjugate  $\frac{\partial \hat{U}^\dagger(t)}{\partial t} = \frac{i}{\hbar} \hat{U}^\dagger(t)\hat{H}(t)$ , it can be shown that:

Operator name	Symbol $\hat{\Omega}$	$\hat{\Omega}^g = \hat{G}\hat{\Omega}\hat{G}^\dagger$
Position	$\hat{X}$	✓
Canonical momentum	$\hat{P}$	✗
Velocity	$\hat{V}$	✓
Position projector	$ x\rangle\langle x $	✓
Canonical momentum projector	$ p\rangle\langle p $	✗
Velocity projector	$ v\rangle\langle v $	✓
Vector Potential	$\hat{\mathcal{A}}$	✗
Scalar Potential	$\hat{A}$	✗
Electric field	$\hat{E}$	✓
Magnetic field	$\hat{B}$	✓
Hamiltonian	$\hat{H}$	✗
Kinetic energy	$\hat{W}$	✓

**Table 1.** Typical operators satisfying (✓) or not (✗) the gauge conditions  $\hat{\Omega}^g = \hat{G}\hat{\Omega}\hat{G}^\dagger$ . The previous condition has to be satisfied by  $\hat{\Omega} = \hat{O}, \hat{\Lambda}$  (i.e., C1, C2) to ensure a gauge-invariant expectation value. Satisfying the previous condition for  $\hat{\Omega} = \hat{O}, \hat{\Lambda}, \hat{F}$  (i.e., C1, C2 and C3) are necessary and sufficient to define a gauge-invariant weak value.

<sup>4</sup>The paper is not dealing with the gauge invariance of a weak value due to an arbitrary (global) phase in quantum states, but with the (electromagnetic) gauge invariance when not only the quantum states are changed as  $|f\rangle \rightarrow |f^g\rangle$  and  $|\psi\rangle \rightarrow |\psi^g\rangle$  as indicated in Eq. (5) with an arbitrary and local phase determined by  $g(x, t)$ , but also the operator is changed as  $\hat{O} \rightarrow \hat{O}^g$  because the electromagnetic potentials have changed in Eq. (3) with the same  $g(x, t)$ .

$$\frac{\partial \mathcal{E}(\hat{O}, t | \psi)}{\partial t} = \langle \Psi(t) | \hat{C} | \Psi(t) \rangle, \quad (9)$$

where we have defined:

$$\hat{C} := \frac{d\hat{O}(t)}{dt} = \frac{i}{\hbar} [\hat{H}, \hat{O}] + \frac{\partial \hat{O}}{\partial t}. \quad (10)$$

As far as the initial state is properly identified by the eigenvalue  $\lambda$ , and the operator  $\hat{O}$  satisfies,  $\hat{O}^g := \hat{G}\hat{O}\hat{G}^\dagger$ , it can be shown that the time derivative of the expectation value is also gauge invariant  $\langle \Psi^g(t) | \hat{C}^g | \Psi^g(t) \rangle = \langle \Psi(t) | \hat{C} | \Psi(t) \rangle$ . See Online Appendix C and also Refs.<sup>52,54</sup>. In summary, no additional condition (apart from C1 and C2) is needed to ensure the gauge invariance of the time derivative of an expectation value.

All the results presented thus far are well-known in the literature. Equation (10) is just the Heisenberg equation of motion of the operator  $\hat{O}$ . When selecting a particular wave function  $|\psi\rangle$ , the expectation value applied to Eq. (10), using position and momentum as operators, leads to the well-known Ehrenfest theorem<sup>70</sup>.

### Time derivative of weak values

Before discussing their time derivatives, we briefly introduce the weak value. As indicated first by Aharonov et al.<sup>1</sup>, additional empirical insights, which are not directly accessible from the expectation value  $\mathcal{E}(\hat{O}, t | \psi)$ , can be obtained in the laboratory when the protocol to measure the expectation values is modified.

The prepared system  $|\psi\rangle$  is allowed to interact with another system, called the meter (or ancilla). During this interaction, the meter and the system become coupled, and the system undergoes a “weak” perturbation that can be modeled by a POVM linked to  $\hat{O}$ . The subsequent measurement of the meter is expected to yield information about the property of the system associated with  $\hat{O}$  due to the previous system-meter coupling.

Up to this point, the procedure follows the general approach used to measure expectation values (using a POVM instead of a PVM) and introduces no novelty. The distinctive aspect of the weak value is that the averaging over the different meter outputs is performed only on a sub-ensemble of the initial states. This sub-ensemble includes only those initial states that yield the specific eigenvalue  $f$  when a *strong* measurement is performed, at a later time, via the PVM of  $\hat{F}$  (i.e.,  $\hat{F}|f\rangle = f|f\rangle$ ).

In Fig. 1a, we have represented the five steps involved in the definition of a weak value. Considering that the initial state  $|\psi\rangle$  defined at  $t = 0$  evolves during a time interval  $t_R$  between the preparation (pre-selection) and the (*weak*) perturbation, modeled by  $\hat{U}_{t_R} := \hat{U}(t_R)$ , and a time interval  $t_L$  between the (*weak*) perturbation and the *strong* measurement (post-selection), modeled by  $\hat{U}_{t_L} := \hat{U}(t_L)$ , the *expectation* value of  $\hat{O}$  conditioned to the fixed eigenstate  $|f\rangle$  is given by:

$$\mathcal{W}(\hat{O}, t_L, t_R | |f\rangle, |\psi\rangle) := \text{Re} \left\{ \frac{\langle f | \hat{U}_{t_L} \hat{O} \hat{U}_{t_R} | \psi \rangle}{\langle f | \hat{U}_{t_L} \hat{U}_{t_R} | \psi \rangle} \right\}. \quad (11)$$

The notation in the left-hand side of Eq. (11) indicates that the weak value  $\mathcal{W}$  is evaluated over the operator  $\hat{O}$  conditioned to the initial state  $|\psi\rangle$  and the final state  $|f\rangle$  (i.e., a property measured through a weak value changes depending on the initial state  $|\psi\rangle$  and/or the final state  $|f\rangle$ ). Notice that  $\hat{U}_{t_L}$  in Eq. (11) is not complex-conjugated because it is a time evolution operator acting on the initial state  $|\psi\rangle$  (not on  $|f\rangle$ ). In other words,  $|f\rangle$  is an eigenstate of  $\hat{F}$  at the final time, not at the initial time.

To justify that the weak value provides *simultaneous* information on the properties linked to the non-commuting operators  $\hat{O}$  and  $\hat{F}$  (or  $\hat{\Lambda}$  and  $\hat{O}$ ), it is required  $t_L \rightarrow 0$  ( $t_R \rightarrow 0$ ). In the literature, the so-called weak value is typically defined as  $\mathcal{W}(\hat{O}, t_L = 0, t_R = 0 | |f\rangle, |\psi\rangle)$ , and given by:

$$\mathcal{W}(\hat{O} | |f\rangle, |\psi\rangle) := \text{Re} \left\{ \frac{\langle f | \hat{O} | \psi \rangle}{\langle f | \psi \rangle} \right\}. \quad (12)$$

When  $[\hat{F}, \hat{O}] = 0$  or  $[\hat{\Lambda}, \hat{O}] = 0$ , we get  $\mathcal{W}(\hat{O} | |f\rangle, |\psi\rangle) = o$  in Eq. (12), where  $o$  is the eigenstate of  $\hat{O}$ . In general, when neither  $[\hat{F}, \hat{O}] = 0$  nor  $[\hat{\Lambda}, \hat{O}] = 0$  is satisfied, the weak value can dramatically differ from an eigenvalue  $o$ , giving additional physical insight about the quantum system. In the rest of the paper, we will use Eqs. (11) or (12) depending on the need to make explicit the time dependence or not of the weak values.

The discussion of the gauge invariance of Eq. (11) requires first that the post-selected eigenvalue  $f$  is gauge invariant (i.e., empirically observable). Using  $|f^g\rangle = \hat{G}|f\rangle$  as in Eq. (5), the eigenvalue equation in an arbitrary gauge  $\hat{F}^g|f^g\rangle = f^g|f^g\rangle$  can be written as  $\hat{F}^g\hat{G}|f\rangle = \hat{G}f^g|f\rangle$ . Thus, to have  $f^g = f$  certifying that the eigenvalue is accessible in the laboratory, the new necessary and sufficient condition on the operator  $\hat{F}$  is

$$\text{C3: } \hat{F}^g := \hat{F}(\hat{\mathcal{A}}^g, \hat{A}^g) = \hat{G}\hat{F}(\hat{\mathcal{A}}, \hat{A})\hat{G}^\dagger,$$

In agreement with Eq. (5), when C3 is satisfied, the direct measurement of  $|f^g\rangle$  is not accessible, but one can infer that the quantum system is  $|f^g\rangle$  (in any gauge) by the measurement of the (gauge invariant) eigenvalue  $f$ . The role played by C3 in identifying  $|f\rangle$  is identical to the role played by C2 in identifying  $|\psi\rangle$ .

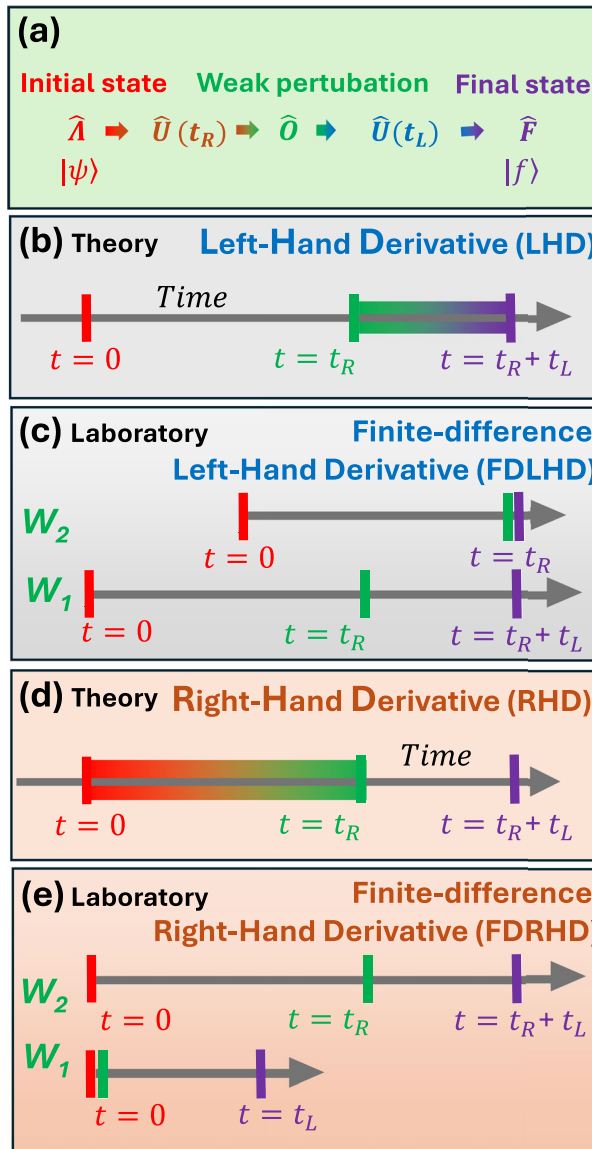


**Fig. 1.** (a) The weak value in Eq. (11) involves five steps: preparation of  $|\psi\rangle$  (red) at the initial time  $t = 0$ , unitary evolution  $\hat{U}_{t_R}$ , weak perturbation linked to  $\hat{O}$  (green) at time  $t = t_R$ , unitary evolution  $\hat{U}_{t_L}$  and strong measurement linked to  $\hat{F}$  (violet) at the final time  $t = t_R + t_L$ . The weak value can be roughly understood as the property of the system during the intermediate green times. (b) The LHD computed when  $t_L \rightarrow 0$  while  $t_R$  is keep constant. (c) The FDLHD is evaluated at the final time and computed from the difference of the weak value  $W_1$  and  $W_2$ , which are computed using two different values of  $t_L$  ( $t_L = 0$  and  $t_L > 0$ ). (d) The RHD computed when  $t_R \rightarrow 0$  while  $t_L$  is keep constant. (e) The FDRHD is evaluated at the intermediate time and computed from the difference of the weak values  $W_1$  and  $W_2$ , which are computed using two different values of  $t_R$  (i.e.,  $t_R > 0$  and  $t_R = 0$ ).

Finally, the gauge invariance of Eq. (11) requires  $\langle f^g | \hat{U}_{t_L}^g \hat{O}^g \hat{U}_{t_R}^g | \psi^g \rangle / \langle f^g | \hat{U}_{t_L}^g \hat{U}_{t_R}^g | \psi^g \rangle = \langle f | \hat{U}_{t_L} \hat{O} \hat{U}_{t_R} | \psi \rangle / \langle f | \hat{U}_{t_L} \hat{U}_{t_R} | \psi \rangle$ . By construction, according to Eqs. (5) and (6), the denominator satisfies  $\langle f | \hat{U}_{t_L} \hat{U}_{t_R} | \psi \rangle = \langle f^g | \hat{U}_{t_L}^g \hat{U}_{t_R}^g | \psi^g \rangle$ . Then, only the gauge invariance of the numerator, i.e.  $\langle f | \hat{U}_{t_L} \hat{O} \hat{U}_{t_R} | \psi \rangle = \langle f^g | \hat{U}_{t_L}^g \hat{O}^g \hat{U}_{t_R}^g | \psi^g \rangle$ , needs to be checked. By the same arguments done in discussing the gauge invariance of  $\mathcal{E}(\hat{O}, t | \psi)$ , we conclude that the necessary and sufficient condition to ensure the gauge invariance of the weak value for any pre-selected  $\langle f |$  and post-selected  $|\psi\rangle$  states is that C1 is satisfied (together with C2 and C3). Thus Table 1 can also be used to discern which operators produce gauge-invariant weak values. Practical examples of gauge-invariant (and gauge-dependent) weak values will be presented in Section “Examples on Gauge invariance of weak values”.

To simplify the discussion, unless indicated, the weak value will be referred only to the real (not complex) value written in Eq. (11). If needed, the weak value can be defined as a real plus an imaginary part,

$\mathcal{W}(\hat{O}, t_L, t_R | f, |\psi\rangle) + i\mathcal{W}_i(\hat{O}, t_L, t_R | f, |\psi\rangle)$ . The imaginary part is identified by a subscript  $i$ , indicating that the experimental measuring protocol to get the (imaginary) weak value  $\mathcal{W}_i$  is different from the experimental measuring protocol to get the (real) weak value  $\mathcal{W}$ . See a detailed discussion in Ref.<sup>71,72</sup>.

As mentioned in the introduction, the time derivative of a physical property frequently gives rise to another meaningful property. We are interested here in the time derivative of a weak value. We also argue in the introduction that there is no consensus on either the ontological meaning of a weak value or the proper protocol to measure them. This lack of consensus will not affect the conclusions of this paper since we are only assuming the mathematical expression of the weak value given by Eq. (11) in all further developments. The weak value in Eq. (11) involves three times  $\{0, t_R, t_R + t_L\}$  separated by two time intervals  $t_R$  and  $t_L$ . Thus, two different time derivatives can be envisioned.

### Left-hand derivative (LHD)

The left-hand derivative (LHD) is evaluated at the final post-selected time ( $t = t_R + t_L$ ), and it captures time-variations of  $\hat{U}_{t_L}$  and  $\hat{O}$  (while  $t_R$  is constant) as shown in Fig. 1b. One can evaluate LHD as:

$$\begin{aligned} LHD := & \left. \frac{\partial \mathcal{W}(\hat{O}, t_L, t_R | f, |\psi\rangle)}{\partial t_L} \right|_{t_L=0} = \mathcal{W}(\hat{C}, 0, t_R | f, |\psi\rangle) \\ & + \text{Re} \left\{ \frac{i}{\hbar} \frac{\langle f | \hat{O} \hat{H} \hat{U}_{t_R} | \psi \rangle}{\langle f | \hat{U}_{t_R} | \psi \rangle} - \frac{i}{\hbar} \frac{\langle f | \hat{O} \hat{U}_{t_R} | \psi \rangle \langle f | \hat{H} \hat{U}_{t_R} | \psi \rangle}{\langle f | \hat{U}_{t_R} | \psi \rangle^2} \right\}, \end{aligned} \quad (13)$$

with  $\hat{C} = \frac{i}{\hbar} [\hat{H}, \hat{O}] + \frac{d\hat{O}}{dt}$  the operator mentioned in Eq. (10). See the detailed demonstration in Online Appendix D.

Certainly, the shape of Eq. (13) is very different from the shape of Eq. (11). Thus, Eq. (13) cannot be understood as a weak value of a property linked to  $\hat{C}$ . In addition, this expression presents a relevant impediment to be defined as a weak value because it is gauge dependent (i.e., empirically unobservable). The term  $\mathcal{W}(\hat{C}, 0, t_R | f, |\psi\rangle)$  in Eq. (13) is gauge invariant, but the terms  $\langle f | \hat{O} \hat{H} \hat{U}_{t_R} | \psi \rangle$  and  $\langle f | \hat{H} \hat{U}_{t_R} | \psi \rangle$  are gauge dependent because they are an inner product of the Hamiltonian which is a gauge-dependent operator as shown in Eq. (4) and in Table 1.

In Online Appendix D we have shown that, in general, Eq. (13) becomes gauge dependent when arbitrary states  $|f\rangle$  are post-selected. However, the gauge dependence of the LHD of a weak value disappears, and it becomes empirically measurable, when we fix the post-selected state as an eigenstate of an operator satisfying

$$\text{C4:} \quad [\hat{O}, \hat{F}] = 0.$$

which means that  $\hat{O}|f\rangle = o|f\rangle$ . Thus, only some very particular states  $|f\rangle$  can be considered as post-selected states to compute LHD. Notice that Online Appendix D shows that C4 is a necessary and sufficient condition for the gauge invariance of LHD. Then, only the term  $\mathcal{W}(\hat{C}, 0, t_R | f, |\psi\rangle)$  remains in Eq. (13) and the LHD of the weak value is also a (gauge invariant) weak value. In particular, under this condition C4, a (gauge invariant) Ehrenfest theorem<sup>70</sup> for weak values can be written as:

$$\left. \frac{\partial \mathcal{W}(\hat{O}, t_L, t_R | f, |\psi\rangle)}{\partial t_L} \right|_{t_L=0} = \mathcal{W}(\hat{C}, 0, t_R | f, |\psi\rangle). \quad (14)$$

If  $t_R = 0$ , the weak value provides simultaneous information on two operators. The fact that  $[\hat{O}, \hat{F}] = 0$  in C4 is compatible with  $[\hat{C}, \hat{F}] \neq 0$  so that the right-hand side of Eq. (14) gives simultaneous information on two non-commuting operators  $\hat{C}$  and  $\hat{F}$ . Wiseman's result on the local velocity<sup>5</sup> can be interpreted as a result of Eq. (14), as seen in detail later in the development of Eq. (25) and in section "Local velocity of particle".

### Right-hand derivative (RHD)

The right-hand derivative (RHD) is evaluated at the initial pre-selection time ( $t = 0$ ), and it captures time-variations of  $\hat{U}_{t_L}$  and  $\hat{O}$  (while  $t_L$  is constant) as shown in Fig. 1d. One can evaluate RHD as:

$$\begin{aligned} RHD := & \left. \frac{\partial \mathcal{W}(\hat{O}, t_L, t_R | f, |\psi\rangle)}{\partial t_R} \right|_{t_R=0} = \mathcal{W}(\hat{C}, t_L, 0 | f, |\psi\rangle) \\ & + \text{Re} \left\{ -\frac{i}{\hbar} \frac{\langle f | \hat{U}_{t_L} \hat{H} \hat{O} | \psi \rangle}{\langle f | \hat{U}_{t_L} | \psi \rangle} + \frac{i}{\hbar} \frac{\langle f | \hat{U}_{t_L} \hat{O} | \psi \rangle \langle f | \hat{U}_{t_L} \hat{H} | \psi \rangle}{\langle f | \hat{U}_{t_L} | \psi \rangle^2} \right\}. \end{aligned} \quad (15)$$

Again, in general, the right-hand side of Eq. (15) does not have the shape of a weak value, and it is also gauge dependent. See the detailed demonstration in Online Appendix E. The condition to achieve the gauge invariance of the RHD is

$$\text{C5:} \quad [\hat{O}, \hat{\Lambda}] = 0.$$

which means that  $|\psi\rangle$  is prepared at  $t = 0$  as an eigenstate of the operator  $\hat{O}$ , i.e.,  $\hat{O}|\psi\rangle = o|\psi\rangle$ . Since the initial state is prepared by detecting an eigenstate  $\lambda$  of the operator  $\hat{\Lambda}$  (as discussed in C2), the operator  $\hat{\Lambda}$  commutes with  $\hat{O}$  as indicated in C5. Notice that it is a necessary and sufficient condition for the gauge invariance of RHD, as shown in Online Appendix E.

Finally, when C5 is satisfied, similarly to what happens to LHD, Eq. (15) for evaluating the RHD can be rewritten as:

$$\left. \frac{\partial \mathcal{W}(\hat{O}, t_L, t_R | f, |\psi\rangle)}{\partial t_R} \right|_{t_R=0} = \mathcal{W}(\hat{C}, t_L, 0 | f, |\psi\rangle). \quad (16)$$

Again, the fact that  $[\hat{O}, \hat{\Lambda}] = 0$  in C5 is compatible with  $[\hat{C}, \hat{\Lambda}] \neq 0$  so that the time-derivative of a weak value in Eq. (16) provides simultaneous information on two non-commuting operators. When conditions C4, C5 are not satisfied, LHD and RHD are different and gauge dependent.

The sum of RHD in Eq. (15) and LHD in Eq. (13), at  $t_R = 0$  and  $t_L = 0$  respectively, gives:

$$\begin{aligned} & \left. \frac{\partial \mathcal{W}(\hat{O}, 0, t_R | f, |\psi\rangle)}{\partial t_R} \right|_{t_R=0} + \left. \frac{\partial \mathcal{W}(\hat{O}, t_L, 0 | f, |\psi\rangle)}{\partial t_L} \right|_{t_L=0} \\ &= \mathcal{W}(\hat{C}, 0, 0 | f, |\psi\rangle) + \frac{\langle f | \frac{\partial \hat{O}}{\partial t} | \psi \rangle}{\langle f | \psi \rangle}. \end{aligned} \quad (17)$$

Notice that Eq. (17) introduces a strong relationship between LHD and RHD. The term  $\mathcal{W}(\hat{C}, 0, 0 | f, |\psi\rangle)$  is gauge invariant. On the contrary, the term  $\langle f | \frac{\partial \hat{O}}{\partial t} | \psi \rangle / \langle f | \psi \rangle$  can be gauge dependent for a time-dependent (Schrödinger picture) operator  $\hat{O}$ . In this paper, we will only consider time-independent operators  $\hat{O}$ . Then, Eq. (17) specifies that if LHD is gauge invariant, then RHD is also gauge invariant, and vice versa.

### Finite-difference approximations

In the laboratory, the time derivative of a weak value can be numerically computed after empirically evaluating two different weak values,  $\mathcal{W}_1$  and  $\mathcal{W}_2$ , which differ in a time interval  $\tau$ . Then, the time derivative can be numerically approximated as the finite difference  $(\mathcal{W}_2 - \mathcal{W}_1)/\tau$ . Again, we can distinguish between a finite-difference left-hand derivative (FDLHD) when  $\tau = t_L$ , as seen in Fig. 1c, and a finite-difference right-hand derivative (FDRHD) when  $\tau = t_R$ , as seen in Fig. 1e.

However, an apparent contradiction arises here because the finite-difference approximation of the time derivative of a weak value discussed in this section is, by construction, always gauge invariant (as long as the weak values  $\mathcal{W}_1$  and  $\mathcal{W}_2$  are gauge invariant by satisfying conditions C1, C2, and C3), while we have shown that LHD and RHD can be gauge dependent (even if conditions C1, C2, and C3 are fully satisfied) when conditions C4 and C5 are not accomplished, as discussed in the previous section.

A proper way to begin addressing the apparent contradiction between theoretical (LHD and RHD) and empirical (FDLHD and FDRHD) time derivatives of weak values is to recall that they are not the same. In quantum mechanics, theoretical properties and empirical properties do not always have a direct connection<sup>5</sup>. The theoretical time derivative is an operation on the Hilbert space, whereas the empirical time derivative is an operation on the empirical weak values of the laboratory. Therefore, if the theoretical LHD and RHD are not conceptually identical to the empirical FDLHD and FDRHD, the gauge behavior of the theoretical and empirical time-derivative of weak values can be different. This point is further elaborated in the following discussion.

### Finite-difference left-hand derivative (FDLHD)

The finite-difference left-hand derivative (FDLHD) is evaluated at the final post-selected time ( $t = t_R + t_L$ ) as happens to LDH. The FDLHD requires the empirical evaluation of the weak value  $\mathcal{W}(\hat{O}, t_L, t_R | f, |\psi\rangle)$  as well as the weak value  $\mathcal{W}(\hat{O}, 0, t_R | f, |\psi\rangle)$ , as depicted in Fig. 1c. Then, the FDLHD for a small  $t_L$  (while  $t_R$  arbitrarily fixed) is:

$$FDLHD := \frac{\mathcal{W}(\hat{O}, 0, t_R | f, |\psi\rangle) - \mathcal{W}(\hat{O}, t_L, t_R | f, |\psi\rangle)}{t_L}. \quad (18)$$

In both weak values, the pre-selected state  $|\psi(0)\rangle$  is prepared at  $t = 0$ . However, the weak perturbation is produced at time  $t = t_R$  in the first weak value and time  $t = t_R + t_L$  in the second. Identically, the (same) post-selected state  $\langle f |$  is considered at  $t = t_R$  in the first weak value and at  $t = t_R + t_L$  in the second. As indicated in Fig. 1c,  $\mathcal{W}(\hat{O}, 0, t_R | f, |\psi\rangle)$  with  $t_L = 0$  provides information on what is the property of the quantum system

<sup>5</sup>For example, the theoretical projective measurement of the eigenvalue  $x$  of the position operators implies that the theoretical wave function collapses into a Dirac delta function. But, this cannot be an exact explanation of what happens in a laboratory when the empirical position  $x$  is measured because a delta function would contain an infinite amount of energy (which cannot be a realistic scenario in a laboratory).

(linked to  $\hat{O}$ ) at the time when the system *is* post-selected in  $\langle f|$ . On the contrary,  $\mathcal{W}(\hat{O}, t_L, t_R | \langle f|, |\psi\rangle)$  provides information on what *was* such property, not at the time when the post-selection  $\langle f|$  takes place, but at a time  $t_L$  earlier. For example, we can expect  $\mathcal{W}(\hat{X}, 0, t_R | \langle f|, |\psi\rangle) > \mathcal{W}(\hat{X}, t_L, t_R | \langle f|, |\psi\rangle)$  for a quantum system with positive velocity.

Let us notice that, apart from Eq. (18), other finite-difference approximations can also be invoked to define a first-order time derivative of Eq. (13). In any case, the FDLHD is obtained by a simple numerical manipulation of the empirical weak values. Thus, the fact that the two empirical weak values involved in Eq. (18) are gauge invariant (as long as conditions C1, C2, and C3 are satisfied) implies that FDLHD itself is gauge invariant too. In Online Appendix F, it is shown that Eq. (18) becomes equal to Eq. (13) when condition C4 is satisfied.

### Finite-difference right-hand derivative (FDRHD)

The finite-difference right-hand derivative (FDRHD), as happens to RHD, is evaluated at the initial (pre-selection) time, i.e.,  $t = 0$ . The FDRHD requires evaluating the following two weak values as seen in Fig. 1e:

$$FDRHD := \frac{\mathcal{W}(\hat{O}, t_L, t_R | \langle f|, |\psi\rangle) - \mathcal{W}(\hat{O}, t_L, 0 | \langle f|, |\psi\rangle)}{t_R}. \quad (19)$$

Again, the pre-selected state  $|\psi(0)\rangle$  is prepared at  $t = 0$ . But, the same post-selected state  $\langle f|$  is evaluated at  $t = t_L + t_R$  in the first weak value and at  $t = t_L$  in the second. Now, as indicated in Fig. 1e, the weak value  $\mathcal{W}(\hat{O}, t_L, 0 | \langle f|, |\psi\rangle)$  with  $t_R = 0$  provides information on what *is* the property of the quantum system (linked to  $\hat{O}$ ) at the time the system *is* pre-selected in  $|\psi\rangle$ , while  $\mathcal{W}(\hat{O}, t_L, t_R | \langle f|, |\psi\rangle)$  provides such information at a time interval  $t_R$  after the system *was* pre-selected in  $|\psi\rangle$ . For example, we can expect  $\mathcal{W}(\hat{X}, t_L, t_R | \langle f|, |\psi\rangle) > \mathcal{W}(\hat{X}, t_L, 0 | \langle f|, |\psi\rangle)$  for a quantum system with positive velocity. Again, both weak values are gauge invariant and observable in the laboratory (as long as conditions C1, C2, and C3 are satisfied). In Online Appendix G, it is shown that FDRHD becomes equal to RHD when condition C5 is satisfied.

As mentioned in the introduction to this section, when conditions C4 and C5 are not satisfied, the LHD and RHD are gauge dependent, whereas the FDLHD and FDRHD remain gauge independent. The physical reason, as explained earlier, is that the former involve operations in the Hilbert space, while the latter are defined in the laboratory frame. The mathematical distinction can be identified in the elements involved in their respective inner products.

By construction, the inner products required for evaluating the FDLHD involve the same inner products needed to evaluate a weak value in Eq. (11). Thus, the relevant elements are the pre- and post-selected states, the  $\hat{O}$  operator, and the time-evolution operators  $\hat{U}_{t_L}$  and  $\hat{U}_{t_R}$ . In contrast, the evaluation of the inner products in the LHD in Eq. (13) involves the same states and  $\hat{O}$  operator but, apart from the time-evolution operators, it also involves explicitly the Hamiltonian operator  $\hat{H}$ . This Hamiltonian operator depends on  $\partial g(x, t)/\partial t$ , as shown in Eq. (4). It is this dependence on  $\partial g(x, t)/\partial t$  that leads to the gauge-dependence of the inner products involving the Hamiltonian<sup>6</sup> (for the same reason, the Hamiltonian has gauge-dependent expectation values as seen in Table 1). In simple terms, the FDLHD in Eq. (18) can be obtained in the laboratory when  $t_L$  is small (but not in the limit  $t_L \rightarrow 0$ ). Thus, it always involves  $\hat{U}_{t_L}$  and  $\hat{U}_{t_R}$  with finite  $t_L$  and  $t_R$ , whose inner products remain gauge invariant. However, defining the LHD in Eq. (13) requires taking the limit  $t_L \rightarrow 0$ , which implies dealing with the inner products that explicitly depend on  $\hat{H}$ , making them gauge dependent when condition C4 is not satisfied. The same reasoning applies to the FDRHD and RHD.

We illustrate these important results with the following numerical simulations.

### Numerical comparison

We consider a particle in free space and we evaluate the weak value of the position and its time derivative (which, in most cases, not all, will mean the velocity). The expressions LHD, RHD, FDLHD, and FDRHD are evaluated using the different Gaussian wave packets listed in Table 2 as pre- and post-selected states. The time derivative of the weak values is computed numerically as explained below.

#### When C4 is satisfied

In Fig. 2a, the pre-selected state is a Gaussian wave packet with a normal (not too short and not too large) spatial dispersion  $|\psi\rangle = |\Phi_1\rangle$ , while the post-selected state is the Gaussian wave packet with a very short spatial dispersion  $\langle f| = \langle \Phi_2|$ , as seen in Table 2. The last Gaussian wave packet is so narrow that it mimics a position eigenstate  $\langle f| = \langle \Phi_2| \approx \langle x_c|$ . The theoretical LHD in Eq. (13) for the position operator  $\hat{O} = \hat{X}$ , when  $t_R = 0$ , can be written as:

<sup>6</sup>The reader can argue that the time-evolution operators  $\hat{U}_{t_L}$  and  $\hat{U}_{t_R}$  in FDLHD also depend on  $\hat{H}$ —which itself includes  $\partial g(x, t)/\partial t$ —as seen in Eq. (6). However, the time integral in Eq. (6) transforms  $\partial g(x, t)/\partial t$  into a gauge function  $g(x, t)$  (without its time derivative). The final dependence of  $\hat{U}_{t_L}$  and  $\hat{U}_{t_R}$  on  $g(x, t_L)$  or  $g(x, t_R)$  in the inner products of FDLHD is unproblematic, as demonstrated in Online Appendix F. The same happens to FDRHD as shown in Online Appendix G.

Wave packet	$E_c$	$k_c$	$v_c$	$x_c$	$\sigma_x$	Observation
	meV	nm <sup>-1</sup>	10 <sup>5</sup> m/s	nm	nm	
$\langle x \Phi_1\rangle$	10	0.132	2.28	400	84	
$\langle x \Phi_2\rangle$	5	0.097	1.61	400	5	$\approx \delta(x - x_c)$
$\langle x \Phi_3\rangle$	10	0.132	2.28	400	60	
$\langle x \Phi_4\rangle$	5	0.097	1.61	400	40	
$\langle x \Phi_5\rangle$	50	0.29	5.12	200	127	$\approx e^{ik_c x}$

**Table 2.** Different Gaussian wave packets  $\langle x|\Phi_i\rangle = \psi_{E_c, x_c, \sigma_x}(x, t_I)$  used in the numerical simulations in this work and defined in Eq. (N50), in Online Appendix N, in terms of the central energy  $E_c$ , central wave vector  $k_c = \sqrt{2m^*E/\hbar^2}$ , central velocity  $v_c = \frac{\hbar k_c}{m^*}$ , central position  $x_c$ , and spatial dispersion  $\sigma_x$  at the wave packet preparation time.

$$\left. \frac{\partial \mathcal{W}(\hat{X}, t_L, 0 || x_c, |\Phi_1\rangle)}{\partial t_L} \right|_{t_L=0} = \mathcal{W}(\hat{V}, 0, 0 || x_c, |\Phi_1\rangle) + Re \left\{ \frac{i}{\hbar} \frac{\langle x_c | \hat{X} \hat{H} | \Phi_1 \rangle}{\langle x_c | \Phi_1 \rangle} - \frac{i}{\hbar} \frac{\langle x_c | \hat{X} | \Phi_1 \rangle}{\langle x_c | \Phi_1 \rangle} \frac{\langle x_c | \hat{H} | \Phi_1 \rangle}{\langle x_c | \Phi_1 \rangle} \right\}. \tag{20}$$

The numerical evaluation of inner products in Eq. (20) just requires multiplying  $|\Phi_1\rangle$  by the operators  $\hat{H}$  and/or  $\hat{X}$  and doing the appropriate inner products with  $\langle \Phi_2 | \approx \langle x_c |$ . The results are plotted in a solid red line in Fig. 2a at  $t_R = t_L = 0$ . Since C4 is satisfied, LHD is given by  $\mathcal{W}(\hat{V}, 0, 0 || v_o, |\psi\rangle) = Re \left\{ \frac{\langle x_c | \hat{V} | \Phi_1 \rangle}{\langle x_c | \Phi_1 \rangle} \right\} = v_B^{|\Phi_1\rangle}(x_c, 0) \approx \hbar k_{c,1}/m^* = 2.28 \cdot 10^5$  m/s which corresponds to the Bohmian velocity of  $\langle x_c | \Phi_1(0) \rangle$ . The formal development leading to the definition of the Bohmian velocity  $v_B^{|\Phi_1\rangle}$  will be elaborated in detail later in the development of Eq. (25) (see also Eq. (27)).

We now evaluate FDLHD following Eq. (18) for different  $t_L$  (and  $t_R = 0$ ) as:

$$\frac{\mathcal{W}(\hat{X}, 0, 0 || x_c, |\Phi_1\rangle) - \mathcal{W}(\hat{X}, t_L, 0 || x_c, |\Phi_1\rangle)}{t_L} \approx \frac{x_c - x_L}{t_L}, \tag{21}$$

where we have defined  $x_c = \mathcal{W}(\hat{X}, 0, 0 || x_c, |\Phi_1\rangle) = Re \left\{ \frac{\langle x_c | \hat{X} | \Phi_1 \rangle}{\langle x_c | \Phi_1 \rangle} \right\} = Re \left\{ \frac{\langle x_c | \hat{X} | \Phi_1 \rangle}{\langle x_c | \Phi_1 \rangle} \right\}$  and  $x_L := \mathcal{W}(\hat{X}, t_L, 0 || x_c, |\Phi_1\rangle) = Re \left\{ \frac{\langle x_c | \hat{U}_{t_L} \hat{X} | \Phi_1 \rangle}{\langle x_c | \hat{U}_{t_L} | \Phi_1 \rangle} \right\}$ . The numerical evaluation of the last weak values requires preparing  $|\Phi_1(0)\rangle$  at the preparation time  $t_1 = 0$  and letting it evolve unitarily during a time interval  $t_L$  following the algorithm described in Eq. (N52) in Online Appendix N. The inner product of the evolved  $|\Phi_1(t_L)\rangle$  with the not-evolved  $\langle \Phi_2(t_L) | \approx \langle x_c |$ , defined at its preparation time  $t_2 = t_L$ , provides the required denominator  $\langle x_c | \hat{U}_{t_L} | \Phi_1 \rangle$ . The numerator i.e.,  $\langle x_c | \hat{U}_{t_L} \hat{X} | \Phi_1(0) \rangle$  requires the time evolution following the algorithm described in Eq. (N52) in Online Appendix N, during the time interval  $t_L$ , of a state defined by the product of  $|\Phi_1(0)\rangle$  by  $\hat{X}$ . The final results in Eq. (21) are plotted in red in Fig. 2a for different values of  $t_L$ . The numerical values of results LHD and FDLHD are roughly identical, as justified in Online Appendix F when C4 is satisfied.

The values of RHD and FDRHD are also computed numerically with similar procedures, giving both values close to zero as plotted in blue in Fig. 2a. Such results can be easily justified through condition Eq. (17) rewritten here as  $LHD + RHD = Re \left\{ \frac{\langle x_c | \frac{i}{\hbar} [\hat{H}, \hat{X}] | \Phi_1 \rangle}{\langle x_c | \Phi_1 \rangle} \right\} = v_B^{|\Phi_1\rangle}(x_c, 0)$ , which fixes RHD to zero because we have already shown that LHD gives  $v_B^{|\Phi_1\rangle}(x_c, 0)$ . The value FDRHD is also zero because it satisfies a similar relationship with FDLHD as shown in Eq. (G36) in Online Appendix G.

Notice that the results in Fig. 2a have been computed for different angles  $\theta$ . These angles  $\theta$  parametrize different gauge functions  $g(x, t)$  as described in Eq. (N56) in Online Appendix N. The initial pre- and post-selected states are the ones mentioned above multiplied by the gauge function at their respective initial time,  $e^{i\frac{\theta}{\hbar} g(x, 0)} \langle x | \Phi_1(0) \rangle$  and  $e^{-i\frac{\theta}{\hbar} g(x, t_L)} \langle \Phi_2(t_L) | x \rangle$ , as described in Eq. (N57) in Online Appendix N and their time evolution is given now by the algorithm described in Eq. (N63) in Online Appendix N. Here, all the final outputs become gauge independent (i.e, they do not depend on the selected gauge function parametrized by the angle  $\theta$ ). The FDLHD and FDRHD are gauge independent by construction, while LHD and RHD are gauge independent here because condition C4 is satisfied.

*When C5 is satisfied*

In Fig. 2b, we plot similar results for a scenario where  $|\psi\rangle$  and  $\langle f|$  are interchanged. The pre-selected state is  $|\psi\rangle = |\Phi_2\rangle \approx |x_c\rangle$ , while the post-selected states is  $\langle f| = \langle \Phi_1|$ . The theoretical RHD in Eq. (15), when  $t_L = 0$ , can be written as:

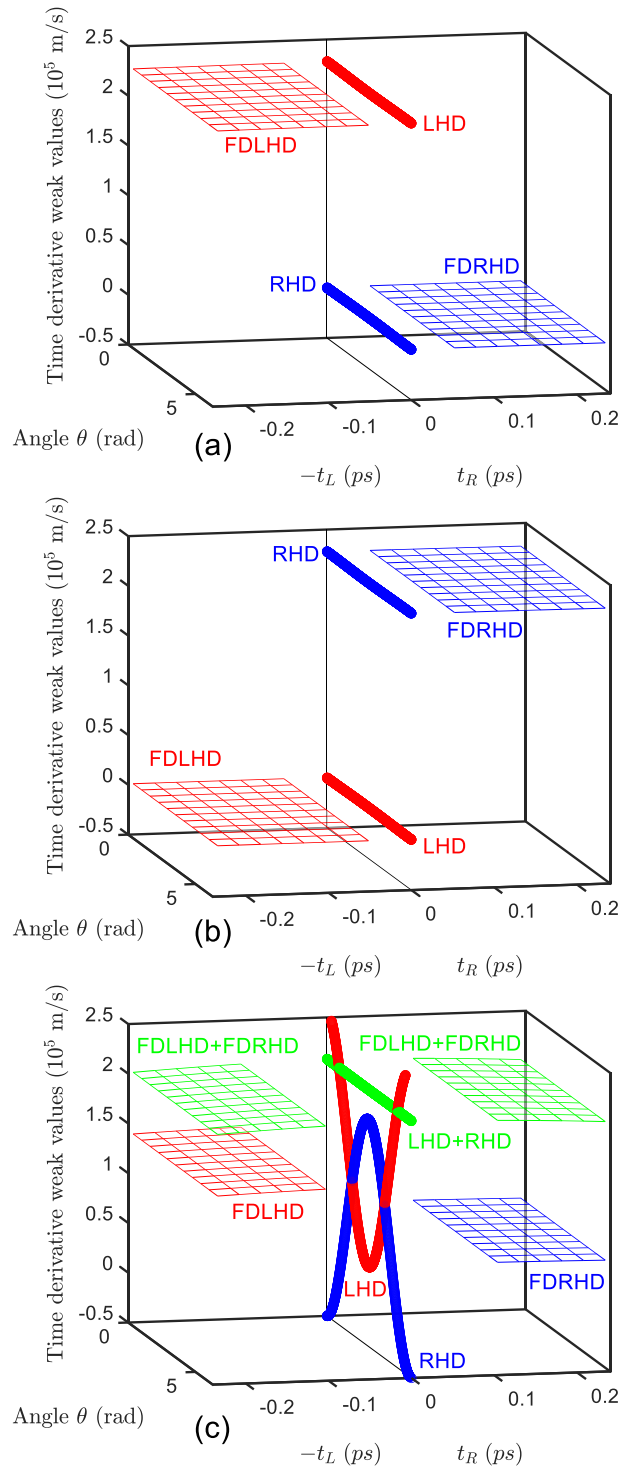


**Fig. 2.** Time derivative of the weak value of the position for different pre- and post-selected states defined in Table 2 at different angles  $\theta$  that parametrize different gauge functions  $g(x, t)$ . At  $t_L = t_R = 0$ , LHD (red) and RHD (blue); at negative  $t_L$ , FDLHD (red); at positive  $t_R$ , FDRHD (blue) are plotted. (a)  $|\Phi_1\rangle$  for the pre-selected state and  $\langle\Phi_2|$  for the post-selected state satisfying condition C4. (b)  $|\Phi_2\rangle$  for the pre-selected state and  $\langle\Phi_1|$  for the post-selected state satisfying condition C5. (c)  $|\Phi_3\rangle$  for the pre-selected state and  $\langle\Phi_4|$  for the post-selected state without satisfying neither condition C4 nor C5. The sum LHD+RHD (green) at  $t_L = t_R = 0$  and FDLHD+FDRHD (green) at positive  $t_R$  and negative  $t_L$  are also plotted.

$$\left. \frac{\partial \mathcal{W}(\hat{X}, 0, t_R | |\Phi_1\rangle, |x_c\rangle)}{\partial t_R} \right|_{t_R=0} = \mathcal{W}(\hat{V}, 0, 0 | |\Phi_1\rangle, |x_c\rangle) \quad (22)$$

$$+ \text{Re} \left\{ -\frac{i}{\hbar} \frac{\langle \Phi_1 | \hat{H} \hat{X} | x_c \rangle}{\langle \Phi_1 | x_c \rangle} + \frac{i}{\hbar} \frac{\langle \Phi_1 | \hat{X} | x_c \rangle \langle \Phi_1 | \hat{H} | x_c \rangle}{\langle \Phi_1 | x_c \rangle \langle f | x_c \rangle} \right\}.$$

Since **C5** is satisfied RHD is given by  $\mathcal{W}(\hat{V}, 0, 0 | |\Phi_1\rangle, |x_c\rangle) = \text{Re} \left\{ \frac{\langle \Phi_1 | \hat{V} | x_c \rangle}{\langle \Phi_1 | x_c \rangle} \right\} = v_B^{|\Phi_1\rangle}(x_c, 0) \approx \frac{\hbar k_{c,1}}{m^*} \approx 2.28 \cdot 10^5$  m/s which corresponds again to the Bohmian velocity of the  $\langle x_c | \Phi_1(0) \rangle$  computed in Fig. 2a. This last result is a consequence of the hermiticity of the  $\hat{V}$ , which implies that  $\text{Re} \left\{ \frac{\langle \Phi_1 | \hat{V} | x_c \rangle}{\langle \Phi_1 | x_c \rangle} \right\} = \text{Re} \left\{ \frac{\langle x_c | \hat{V} | \Phi_1 \rangle}{\langle x_c | \Phi_1 \rangle} \right\}$ .

We also evaluate FDRHD in the laboratory for different  $t_R$  (and  $t_L = 0$ ) following Eq. (19):

$$\frac{\mathcal{W}(\hat{X}, 0, t_R | |\Phi_1\rangle, |x_c\rangle) - \mathcal{W}(\hat{X}, 0, 0 | |\Phi_1\rangle, |x_c\rangle)}{t_R} \approx \frac{x_R - x_c}{t_R}, \quad (23)$$

where we have defined  $x_c = \mathcal{W}(\hat{X}, 0, 0 | |x_c\rangle, |\Phi_1\rangle) = \text{Re} \left\{ \frac{\langle x_c | \hat{X} | \Phi_1 \rangle}{\langle x_c | \Phi_1 \rangle} \right\}$  and  $x_R := \mathcal{W}(\hat{X}, 0, t_R | |x_c\rangle, |\Phi_1\rangle) = \text{Re} \left\{ \frac{\langle x_c | \hat{X} \hat{U}_{t_R} | \Phi_1 \rangle}{\langle x_c | \hat{U}_{t_R} | \Phi_1 \rangle} \right\}$ . The numerical evaluation of the second weak value implies preparing  $|\Phi_2(0)\rangle \approx |x_c\rangle$  at the preparation time  $t_2 = 0$  and allowing the system to evolve unitarily during a time interval  $t_R$  following the evolution described in Eq. (N52) in Online Appendix N. The inner products are done in a similar way as described for Fig. 2a, involving now  $\langle \Phi_1(t_R) |$  at the preparation time  $t_1 = t_R$ . In Fig. 2b, in blue, we show that the results RHD and FDRHD are roughly identical. The condition Eq. (17) and Eq. (G36) also fix the values of LHD and FDLHD to roughly zero. The reasons for the gauge invariance (independence of  $\theta$ ) are equivalent to the ones explained for Fig. 2a. Now, the accomplishment of condition **C5** is involved.

#### When **C4** and **C5** are not satisfied

The next analysis provided in Fig. 2c explores a different scenario where neither the pre-selected state  $|\Phi_3\rangle$  nor the post-selected state  $\langle \Phi_4 |$  can be considered position eigenstates. Thus, since neither condition **C4** nor **C5** is satisfied, the LHD computed from Eq. (20) and RHD computed from Eq. (22) are gauge dependent as seen for the red and blue curves at  $t_L = t_R = 0$ , i.e., their values depend on the angle  $\theta$  which parametrizes different gauge functions  $g(x, t)$  as described in Eq. (N56) in Online Appendix N. On the contrary, by construction, the FDLHD computed from Eq. (21) and FDRHD computed from Eq. (23) remain gauge invariant as described in Online Appendices F and G but their values coincide neither with the Bohmian velocity of  $|\Phi_3\rangle$  nor  $\langle \Phi_4 |$  written in Table 2.

In green, we have plotted LHD+RHD at  $t_R = t_L = 0$  and FDLHD+FDRHD for different values of  $t_L$  and  $t_R$  and  $\theta$ . Both sums become equal and gauge invariant as indicated in Eq. (17) and Eq. (G36) (for the time-independent operator  $\hat{X}$ ), but the value of the sum does not coincide with the sum of the Bohmian velocities. In summary, when neither condition **C4** nor **C5** are satisfied, LHD and RHD cannot be obtained in the laboratory. On the contrary, FDLHD and FDRHD can be empirically evaluated in the laboratory, but it is not clear which physical insight can be attributed to them.

Finally, it is interesting to revisit Eq. (21) to acquire an intuitive motivation for **C4**. It seems *natural* to define the time derivative of a weak value as the difference between two weak values: one weak value  $x_c$  evaluated without time evolution, i.e.,  $\hat{U}_{t_L} = \mathbb{1}$ , and the other weak value  $x_L$  with a time evolution during the time interval  $t_L$ . It seems obvious to define the post-selected position  $x_c$ , when  $\hat{U}_{t_L} = \mathbb{1}$  in terms of weak values as  $x_c = \langle x_c | \hat{X} | \psi \rangle / \langle x_c | \psi \rangle$  with  $\hat{X} | x_c \rangle = x_c | x_c \rangle$ . Thus, the weak value  $x_L$  with arbitrary  $\hat{U}_{t_L}$  has to be defined as  $x_L = \langle x_c | \hat{U}_{t_L} \hat{X} | \psi \rangle / \langle x_c | \hat{U}_{t_L} | \psi \rangle$ , and we conclude that **C4** becomes a quite *natural* requirement for the time derivative of a weak value because the condition  $\hat{X} | x_c \rangle = x_c | x_c \rangle$ , i.e.  $[\hat{O}, \hat{F}] = 0$  for  $\hat{O} = \hat{X}$  and  $\hat{F} = \hat{X}$ , is required at the origin of this argumentation. This is exactly what happens for the LHD in Eq. (13) when **C4** is satisfied. An identical conclusion occurs for **C5** from Eq. (23). All these results regarding the gauge condition and the shape of the theoretical, LHD and RHD, and empirical, FDLHD and FDRHD, weak values are summarized in Table 3.

### Examples on Gauge invariance of weak values

After the theoretical development and finite-difference approximations done in Sections “Time Derivative of Weak values” and “Finite-difference approximations”, here, we show several weak values often mentioned in the literature. In particular, we discuss whether or not they satisfy the gauge invariance implicit in properties **C1**, **C3**. To simplify the discussion, we will assume that the condition **C2** in the preparation of the initial state  $|\psi^g\rangle$  is always satisfied. Since this section does not deal with time-derivative yet, we will use Eq. (12) for the evaluation of the weak values, rather than Eq. (11).

To properly understand the results in this section, first, we need to clarify what we mean when we say, for example, that the canonical momentum on Table 1 is not empirically observable in the laboratory because it is gauge dependent. It is well-known that the canonical momentum  $\hat{P}^g := \hat{P}(\hat{A}^g, \hat{A}^g) = \hat{P} \neq \hat{G}\hat{P}\hat{G}^\dagger$  does not satisfy condition **C1**. Thus, strictly speaking, it cannot be empirically measured in the laboratory either from an expectation value or from a weak value in a direct way. However, in many experimental works, the measurement of the “momentum” is inferred from the measurement of another property that is gauge invariant. For example, by measuring the position of the quantum system on the screen<sup>73</sup> and knowing the initial and final time of the

	Type	Condition	Gauge Inv.	Weak value	Similarity
Theoretical	LHD	C4	✓	✓	≈ FDLHD
		<del>C4</del>	✗	✗	
	RHD	C5	✓	✓	≈ FDRHD
		<del>C5</del>	✗	✗	
Empirical	FDLHD	C4	✓	✓	≈ LHD
		<del>C4</del>	✓	✗	
	FDRHD	C5	✓	✓	≈ RHD
		<del>C5</del>	✓	✗	

**Table 3.** Theoretical (LHD and RHD) and empirical (FDLHD and FDRHD) time-derivative of weak values satisfying (✓) or not (✗) being invariant under gauge transformations (column **Gauge. Inv.**) and having the mathematical shape of a wave value (column **Weak Value**) as a function of the accomplishment or not of conditions **C4** or **C5**. The scenarios when LHD ≈ FDLHD and RHD ≈ FDRHD are indicated (column **Similarity**).

experiment. As we will discuss below, this measuring procedure is a measurement of the velocity (or the velocity multiplied by the mass) rather than a direct measurement of the canonical momentum (we emphasize that the above discussions and all the results in this paper about non-measurable gauge-dependent results do not imply ontological consequences for the canonical momentum or other gauge-dependent properties.).

In other words, the fact that the electromagnetic potentials are not gauge invariant does not imply that they are not physically relevant<sup>51</sup>, but only that they cannot be directly measured in the laboratory.

**Weak value of the canonical momentum post-selected in position**

As discussed above, the canonical momentum operator  $\hat{P}^g := \hat{P}(\hat{\mathcal{A}}^g, \hat{A}^g) = \hat{P} \neq \hat{G}\hat{P}\hat{G}^\dagger$  does not satisfy condition **C1** and cannot be measured through weak values. Let us confirm this point by writing the theoretical expression corresponding to the weak measurement of the canonical momentum plus a subsequent strong measurement of the position operator  $\hat{X}^g := \hat{X}(\hat{\mathcal{A}}^g, \hat{A}^g) = \hat{X} = \hat{G}\hat{X}\hat{G}^\dagger$ . Such weak value would be given by  $\mathcal{W}(\hat{P}|x, |\psi\rangle)$  which, when written in any gauge, becomes

$$Re \left\{ \frac{\langle x^g | \hat{P} | \psi^g \rangle}{\langle x^g | \psi^g \rangle} \right\} = Re \left\{ -i\hbar \frac{\nabla \psi^g}{\psi^g} \right\} = \nabla S - q\nabla g. \tag{24}$$

where  $[\hat{G}, \hat{X}] = 0$  and  $|\psi^g\rangle = \hat{G}|\psi\rangle$ . We use  $\psi(x, t) = R(x, t)e^{iS(x, t)/\hbar}$  in polar form to better elaborate  $\nabla \psi^g / \psi^g$ . The explicit dependence of Eq. (24) on  $\nabla g$  confirms that this weak value cannot be observed in the laboratory.

In the Coulomb gauge representation ( $g = 0$  and  $\nabla \cdot \mathcal{A} = 0$ ), in the absence of a magnetic field  $\mathcal{A} = 0$ , the velocity and canonical momentum operators are identical  $m\hat{V} = \hat{P}$ . This coincidence in one particular gauge does not mean that the velocity and momentum operators are the same in general, i.e.,  $m\hat{V}^g \neq \hat{P}^g$ . In the same way, the knowledge of  $\mathcal{A} = 0$  in the Coulomb gauge does not mean that one can assume  $\mathcal{A}^g = 0$  in another gauge.

**Weak value of the velocity post-selected in position**

Contrary to the canonical momentum, the velocity operator  $\hat{V}^g$  is defined as

$$\hat{V}^g := \hat{V}(\hat{\mathcal{A}}^g, \hat{A}^g) = (\hat{P}^g - q\hat{\mathcal{A}}^g)/m = \hat{V} = \hat{G}\hat{V}\hat{G}^\dagger,$$

and it is gauge invariant and satisfies **C1** for  $\hat{O} = \hat{V}$ . Hence, the weak measurement of the velocity post-selected in position gives the empirically observable weak value  $\mathcal{W}(\hat{V}|x, |\psi\rangle)$  defined as

$$Re \left\{ \frac{\langle x | \hat{V}^g | \psi^g \rangle}{\langle x | \psi^g \rangle} \right\} = \frac{1}{m^*} Re \left\{ -i\hbar \frac{\nabla \psi^g}{\psi^g} - q\mathcal{A}^g \right\} = \frac{\nabla S - q\nabla G^g - q\mathcal{A} + q\nabla G^g}{m^*} := \mathbf{v}_B^{|\psi\rangle}. \tag{25}$$

The weak value gives the so-called Bohmian velocity<sup>5,6,9</sup>,  $\mathbf{v}_B^{|\psi\rangle} = (\nabla S - q\mathcal{A})/m^*$ , which is gauge invariant because it satisfies **C1** for  $\hat{O} = \hat{V}$  and **C3** for  $\hat{F} = \hat{X}$ . See an alternative demonstration in Online Appendix **H** and also<sup>74</sup>. The superscript  $|\psi\rangle$  in  $\mathbf{v}_B^{|\psi\rangle}$  just indicates that the Bohmian velocity is a functional of the wave function  $\psi$ .

As discussed previously (see<sup>71,72</sup>), another weak value can be designed to give the imaginary part of Eq. (25),  $Im\langle x | \hat{V}^g | \psi^g \rangle / \langle x | \psi^g \rangle$ , which is called the “osmotic” velocity  $\mathbf{v}_O^{|\psi\rangle}$ <sup>9,58,75,76</sup> and given by

$v_O^{|\psi\rangle} := -Im\langle x|\hat{V}^g|\psi^g\rangle/\langle x|\psi^g\rangle = \frac{\hbar}{m^*} \frac{\nabla R^g}{R^g}$ , which is also gauge invariant because  $R^g = R$ . Notice that there is some ambiguity regarding the sign in the definition of osmotic velocity in the literature<sup>9,58,75,76</sup>.

The consistency in interpreting  $\mathcal{W}(\hat{V}^g||x\rangle, |\psi\rangle)$  as a velocity is provided by the LHD in Eq. (13) when  $\hat{O} = \hat{X}$  and  $|f\rangle = |x\rangle$ , as will be seen in Eq. (27) in next section.

### Weak value of the position projector post-selected in the canonical momentum

Let us now analyze the weak value corresponding to the position projector  $|x^g\rangle\langle x^g| = \hat{G}^g|x\rangle\langle x|\hat{G}^g = |x\rangle\langle x|$  post-selected by the canonical momentum operator  $\hat{P}$  defined as:

$$\mathcal{W}(|x\rangle\langle x||p\rangle, |\psi\rangle) = \frac{\langle p^g|x\rangle\langle x|\psi^g\rangle}{\langle p^g|\psi^g\rangle}.$$

It is argued in the literature<sup>36,37</sup> that such a weak value, together with the corresponding conditional ensemble for the imaginary part<sup>71,72</sup>, is proportional to the wave function  $\langle x|\psi^g\rangle$  when post-selected at zero momentum. Despite the fact that this weak value satisfies C1 for  $\hat{O} = |x\rangle\langle x|$ , the selection  $\hat{F} = \hat{P}^g$ , to define  $\langle p^g|$ , does not satisfy C3 because the canonical momentum is gauge dependent. The gauge-dependent eigenstate  $\langle x|p^g\rangle = e^{i(qg(x,t)+px)/\hbar}$  has a gauge-dependent eigenvalue  $-i\hbar\nabla\langle x|p^g\rangle = (g(x,t) + p)\langle x|p^g\rangle$ . Thus, this weak value of the canonical momentum cannot be obtained in the laboratory.

### Weak value of the position projector post-selected in the velocity

It is true, however, that the non-measurability of the canonical momentum described above can be avoided by substituting  $\hat{P}$  by  $\hat{V}$ . Then,  $\mathcal{W}(\hat{X}||v\rangle, |\psi\rangle)$ , is given by

$$\frac{\langle v^g|x\rangle\langle x|\psi^g\rangle}{\langle v^g|\psi^g\rangle} = \frac{R_v R_\psi e^{i\frac{S_v - S_\psi}{\hbar}}}{\langle v|\psi\rangle}, \quad (26)$$

where  $\langle v^g|x\rangle = R_v e^{i(S_v + qG)/\hbar}$  and  $\langle x|\psi^g\rangle = R_\psi e^{i(S_\psi + qG)/\hbar}$ . Clearly, this weak value satisfies C1 for  $\hat{O} = |x\rangle\langle x|$  and C3 for  $\hat{F} = \hat{V}$ . Hence, the (phase of the) weak value  $\mathcal{W}(\hat{X}||v\rangle, |\psi\rangle)$  is now gauge invariant, as seen here:  $S_v^g - S_\psi^g = S_v - qG - S_\psi + qG = S_v - S_\psi$ .

However, arguing that Eq. (26) measures the (phase of the) Hilbert space representation of the wave function  $\langle x|\psi^g\rangle$  is not rigorous, because all wave functions are gauge dependent and unmeasurable, as seen in Eq. (5). The argument in the literature is based on assuming that for a magnetic field equal to zero, in the Coulomb gauge,  $m\hat{V} = \hat{P}$  with  $\langle v|x\rangle \propto e^{i(px)/\hbar}$  and  $\langle x|\psi\rangle = R_\psi e^{iS_\psi/\hbar}$ . Then, Eq. (26) gives  $\mathcal{W}(|x\rangle\langle x||v\rangle, |\psi\rangle)_{v=0} \propto \langle x|\psi\rangle$

<sup>36</sup>. While this protocol, which effectively gives the wave function defined in the Coulomb gauge, can indeed be very useful for developing new quantum technologies, there is no reason to affirm that the Coulomb gauge representation of the wave function is the *true* wave function of the system, in the same way as the Coulomb-gauge representation of the electromagnetic potentials are not the *true* potentials. At the fundamental level, there should be no preferred gauge, and hence, the wave function and the potentials are unmeasurable, as indicated in Eqs. (3) and (5), respectively.

### Examples on the time derivative of weak values

Here, we discuss three examples of the time derivative of weak values, dealing with local velocity, the local energy theorem, and the local Lorentz force. These numerical examples explicitly demonstrate the usefulness and abilities of time-dependent weak values.

We compute the time derivative of the weak value through numerical simulations. As discussed in Online Appendix N, the numerical simulations require spatial and temporal grids. Thus, strictly speaking, the time derivatives computed in this section correspond to the finite-difference expressions FDLHD and FDRHD outlined in Section “Finite-difference approximations”. In all simulations, we consider scenarios where conditions C4, C5, or both are satisfied so that the FDLHD and FDRHD can be interpreted as the LHD and RHD defined in Section “Time Derivative of Weak values”. In addition, in these numerical simulations, the time step is chosen to be sufficiently small so that the FDLHD and FDRHD provide excellent approximations to the LHD and RHD (the small numerical time step used in the numerical computations in this paper does not need to coincide with the experimental time step required to evaluate the time derivatives in the laboratory, which must be determined by the time interval over which relevant time-dependent variations occur in the quantum system).

To gain additional physical insight into the behavior of such weak values and their time derivatives, after the numerical evaluation of the weak values, we re-interpret the results as Bohmian properties of a quantum system.

### Local velocity of particle

Wiseman formulated the first attempt to discuss time derivatives of weak values<sup>5</sup> when presenting a local velocity from the time-derivative of a weak value of the position (post-selected in position eigenstates).

In Eq. (25) we have found how the expression  $\mathcal{W}(\hat{V}^g||x\rangle, |\psi\rangle)$  can be interpreted as the local velocity of a quantum particle. The consistency in interpreting  $\mathcal{W}(\hat{V}^g||x\rangle, |\psi\rangle)$  as a velocity is provided by the LHD in Eq. (13) when  $\hat{O} = \hat{X}$  and  $|f\rangle = |x\rangle$ .

$$\left. \frac{\partial \mathcal{W}(\hat{X}, t_L, 0 | |x\rangle, |\psi\rangle)}{\partial t_L} \right|_{t_L=0} = \mathcal{W}(\hat{V}, 0, 0 | |x\rangle, |\psi\rangle), \quad (27)$$

where  $\hat{V} = \frac{i}{\hbar} [\hat{H}, \hat{X}]$  as seen in Online Appendix I. Notice that Eq. (27) satisfies C4 (gauge invariance) because  $[\hat{O}, \hat{F}] = [\hat{X}, \hat{X}] = 0$ . Thus, the local velocity can be obtained for an arbitrary pre-selected quantum state  $|\psi\rangle$  because the condition C4 just fixes the post-selected state  $\langle f | = \langle x |$ . We only require a Hamiltonian that satisfies  $\hat{V} = \frac{i}{\hbar} [\hat{H}, \hat{X}]$ .

As suggested by Wiseman<sup>5</sup>, Eq. (27) shows that the Bohmian velocity is just the quantum version of the classical time-of-flight procedure to evaluate the velocity: two positions are consecutively measured and the velocity defined as the distance divided by the time interval between the two measurements. In the discussion at the end of Section “Finite-difference approximations”, we have identified the first weak value as  $x_c = \langle x_c | \hat{X} | \psi \rangle / \langle x_c | \psi \rangle$  and the second as  $x_L = \langle x_c | \hat{U}_{t_L} \hat{X} | \psi \rangle / \langle x_c | \hat{U}_{t_L} | \psi \rangle$ . Notice that  $\langle x_c | \hat{U}_{t_L} \hat{X} | \psi \rangle / \langle x_c | \hat{U}_{t_L} | \psi \rangle$  can be understood as giving insight on which *was* the (weak value of the) position of the system at a time  $t_L$  earlier than the time when the (strong) position of the system *is*  $x_c$ . This reasoning implies  $x_c = x_L + v_B t_L$  giving  $(x_c - x_L) / t_L = v_B$ , as seen from Eq. (21).

### Local work-energy theorem

The weak value of the Hamiltonian operator in Eq. (1) is not measurable, because  $\hat{H}$  does not satisfy C1 as seen in Eq. (4). On the contrary, the kinetic energy operator defined as  $\hat{W} := \frac{1}{2} m \hat{V}^2$  is gauge invariant. Then, we can use Eq. (15) to compute its RHD as:

$$\left. \frac{\partial \mathcal{W}(\hat{W}, 0, t_R | |x\rangle, |v\rangle)}{\partial t_R} \right|_{t_1=0} = q v_B^{(v)}(x) \cdot E(x), \quad (28)$$

where the operator  $\hat{W}$  is gauge invariant and satisfies C5 because  $|v\rangle$  is an eigenstate of  $\hat{O} = \hat{W}$ . The details can be found in Online Appendices J and K. The expression (28) is just the local version (i.e.,  $x$ -density) of the corresponding global work-energy theorem. If  $q v_B^{(v)}(x) \cdot E(x)$  is positive at some particular location  $x$ , one can interpret that the kinetic energy of the particle at such position increases, while decreases otherwise.

### Numerical example

We show how an example of Eq. (28) can be implemented in a practical scenario. We consider a single electron with a uniform electric field in the  $x$ -direction,  $E = (E, 0, 0)$  with  $E = -1 \cdot 10^6$  V/m. To proceed, we need to find a gauge potential for  $\mathcal{A}$  and  $A$ . There is, of course, no unique choice. We select the usual Coulomb gauge  $\mathcal{A}^g = 0$  and  $A^g = -Ex$ . Since the system becomes separable, to predict the electrical field from the time derivative of a weak value Eq. (28), we can focus only on the  $x$  component of such a weak value. Then, the 1D version of the Hamiltonian in Eq. (1) becomes just:

$$H = H(\mathcal{A}, A) = -\frac{\hbar^2}{2m^*} \frac{\partial^2}{\partial x^2} + qEx, \quad (29)$$

To evaluate RHD (in fact FDRHD), the initial (pre-selected) state has to be an eigenstate of the velocity operator that satisfies C5. We roughly approximate such eigenstate by the Gaussian  $\langle x | \Phi_5(0) \rangle$  described in Table 2. The wave packet spatial dispersion  $\sigma_x = 127$  nm corresponds to a width in the reciprocal space  $\sigma_k = 1/\sigma_x = 7.8 \mu\text{m}^{-1}$ . Thus, the wave packet with a large spatial dispersion  $\sigma_x \rightarrow \infty$  ( $\sigma_k \rightarrow 0$ ) mimics a plane wave, which is an effective eigenstate of the velocity operator.

The numerical time-evolution of  $\langle x | \Phi_5(t) \rangle$  is computed from Eq. (N52) in Online Appendix N. In Fig. 3, we have plotted the time-evolution of modulus squared of  $\langle x | \Phi_5(t) \rangle$  (blue) together with the time-independent potential energy profile (green) as  $qEx$  in Eq. (29). For a posterior discussion, we also plot the Bohmian trajectories  $x_B^j(t)$  for  $j = 1, \dots, N$  computed following the numerical algorithm from Eq. (N55) in Online Appendix N. The velocity of each trajectory can be evaluated from the  $x$ -component of the weak value  $v_B^{(v)} = \{v_{B,x}^{(v)}, v_{B,y}^{(v)}, v_{B,z}^{(v)}\}$  in Eq. (25). In this example, to simplify the notation, we refer to this  $x$ -component of the velocity as  $v_B^{(v)}$ .

In Fig. 4, we have plotted in blue the  $x$ -component of the weak value of the kinetic energy at different times:

$$\mathcal{W}(\hat{W}_x, 0, t_R | |x\rangle, |\Phi_5\rangle) = \text{Re} \left\{ \frac{\langle x | \frac{1}{2} m^* \hat{V}_x^2 \hat{U}_{t_R} | \Phi_5(t) \rangle}{\langle x | \hat{U}_{t_R} | \Phi_5(t) \rangle} \right\}. \quad (30)$$

with  $\hat{W}_x = \frac{1}{2} m^* \hat{V}_x^2$ . The inner products in Eq. (30), i.e.  $\langle x | \frac{1}{2} m^* \hat{V}_x^2 \hat{U}_{t_R} | \Phi_5(t) \rangle$  and  $\langle x | \hat{U}_{t_R} | \Phi_5(t) \rangle$ , are computed in the same way as explained in Section “Numerical comparison”. In orange, the  $x$ -component of the Bohmian velocity, i.e., the weak value in Eq. (25) or in Eq. (27), is also plotted as a function of time.

Finally, in Fig. 5, the time derivative of Eq. (30) shown in Fig. 4 in blue is also plotted. In orange, we plot the estimation of the electrical field  $E = E(x, t)$  from Eq. (28) as

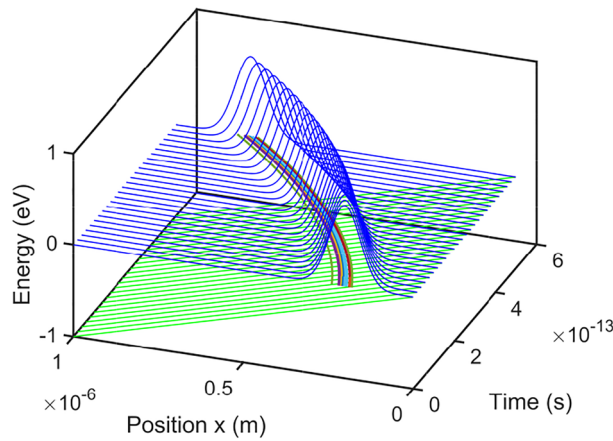


**Fig. 3.** Time evolution of the modulus squared of  $\langle x | \Phi_5(t) \rangle$  (blue) in a time-independent potential energy profile (green). Different Bohmian trajectories  $x_B^j(t)$  for  $j = 1, \dots, 10$  are computed by integrating the  $x$ -component of the weak value of the velocity in Eq. (25) as indicated in Eq. (N55) in Online Appendix N. The different  $x_B^j(t)$  will be used later to evaluate the weak values in different relevant positions and times.

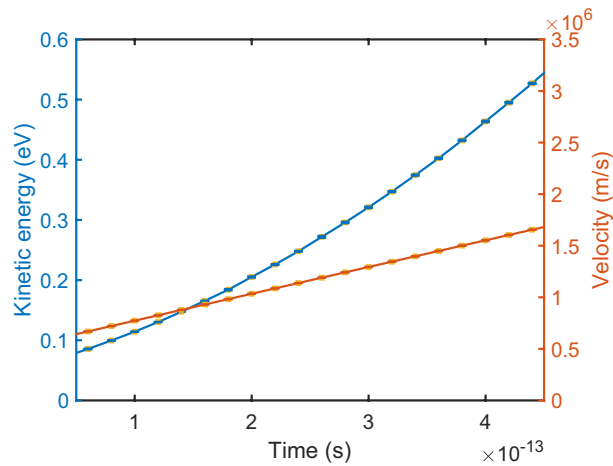


**Fig. 4.** In blue, mean value and standard deviation of the  $x$ -component of the weak value of the kinetic velocity of the 10 trajectories plotted in Fig. 3 at 20 different times computed from Eq. (28) (left axis). In orange, the mean value and standard deviation of the  $x$ -component of the weak value of the velocity in Eq. (25) of the 10 trajectories in Fig. 3 at 20 different times (right axis), which corresponds to the velocity  $v_B^{|\Phi_5\rangle}(t)$ .

$$E(x, t) \approx \left\{ \frac{\frac{\partial}{\partial t_R} Re \left\{ \frac{\langle x | \frac{1}{2} m^* \dot{V}_x^2 \dot{U}_{t_R} | \Phi_5(t) \rangle}{\langle x | \dot{U}_{t_R} | \Phi_5(t) \rangle} \right\}}{q v_B^{|\Phi_5\rangle}(x, t)} \right\}, \tag{31}$$

There is an excellent agreement between the electric field used in this numerical simulation, i.e.,  $E = -1 \cdot 10^6$  V/m, and the value predicted through Eq. (31). As mentioned, and as would also happen in a laboratory, in this numerical simulation the time derivative  $\frac{\partial}{\partial t_R} Re \left\{ \frac{\langle x | \frac{1}{2} m^* \dot{V}_x^2 \dot{U}_{t_R} | \Phi_5 \rangle}{\langle x | \dot{U}_{t_R} | \Phi_5 \rangle} \right\}$  is done through FDRHD in Eq. (19), instead of RHD, as they both give identical results because C5 is satisfied.

Despite one position  $x$  and one time  $t$  being enough to predict  $E(x, t)$  through Eq. (31), we have enriched the figures by considering several times  $t$  and positions  $x$  where the weak values are computed. At each time,  $t$ , the value  $E(x, t)|_{x=x_B^j(t)}$  are numerically evaluated for a set of positions  $x = x_B^j(t)$ , where  $x_B^j(t)$  are the different  $j = 1, \dots, 10$  Bohmian trajectories plotted in Fig. 3. The initial positions of the trajectories are selected according to the initial wave function probability distribution to ensure that they are relevant positions in this scenario at all times. The mean value and the standard deviation of  $E(x, t)|_{x=x_B^j(t)}$  for different times are indicated in Fig. 5. The same procedure is done in Fig. 4 to plot the mean value and the standard deviation of the weak values of the velocity and of the kinetic energy. The information on the standard deviation shows how robust the

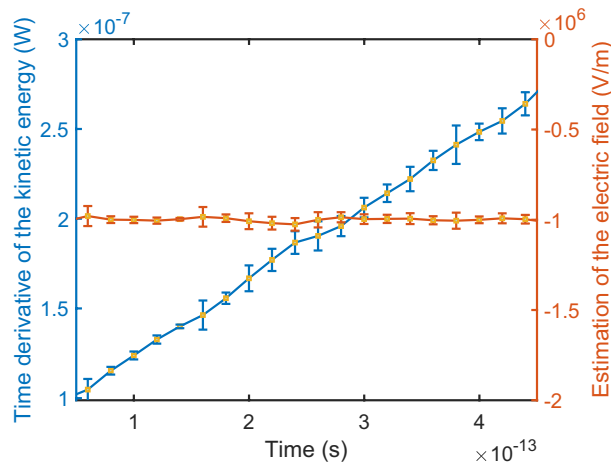


**Fig. 5.** In blue, mean value and standard deviation of the time derivative of Eq. (30) of the 10 trajectories in Fig. 3 at 20 different times (left axis). In orange, the mean value and standard deviation of the electrical field of the 10 trajectories in Fig. 3 at 20 different times computed from Eq. (28) (right axis).

predictions are when different times and positions are considered in this example with a uniform and constant electric field.

We emphasize that the velocity at each position  $x$  and time  $t$  in the trajectories of Fig. 3 requires a specific weak measurement protocol that is independent of previous positions and times. In the laboratory, the computation of the weak value at each time  $t$  would assume that the initial (pre-selected) Gaussian wave packet is defined at such time  $t$ , i.e., the pre-selected state at  $t$  is  $\langle x | \Phi_5(t) \rangle$ . Therefore, the connection of different velocities in Fig. 4 to construct the continuous Bohmian trajectory shown in Fig. 3 is natural within the Bohmian interpretation. However, such a connection is not necessary in the ontologically-free approach used to develop the time-derivative weak values presented in this paper. In any case, it can be illustrative to provide an additional justification of the above results from a Bohmian perspective. The weak value of the kinetic energy in Eq. (30) can be rewritten in a Bohmian language as:

$$Re \left\{ \frac{\langle x | \frac{1}{2} m^* \hat{V}_x^2 | \Phi_5 \rangle}{\langle x | \Phi_5 \rangle} \right\} = \frac{1}{2} m^* \left( v_B^{|\Phi_5\rangle}(x, t) \right)^2 + Q^{|\Phi_5\rangle}(x, t) \approx \frac{1}{2} m^* \left( v_B^{|\Phi_5\rangle}(x, t) \right)^2 \quad (32)$$

where  $Q^{|\Phi_5\rangle}(x, t)$  is the so-called (Bohmian) quantum potential that depends on the curvature of the modulus of the wave function  $\langle x | \Phi_5(t) \rangle$ . For the spatially large wave packet considered here, such a last contribution can be neglected in front of the first one. Then, the last term in Eq. (32) shows one possible procedure to evaluate the weak value of the kinetic energy in Eq. (30) for this particular scenario in the laboratory: once the velocity  $v_B^{|\Phi_5\rangle}(x, t)$

is computed, the kinetic energy  $\frac{1}{2} m^* \left( v_B^{|\Phi_5\rangle}(x, t) \right)^2$  in Eq. (32) can be obtained by numerical post-processing the empirically obtained Bohmian velocity by squaring the value and multiplying the result by  $\frac{1}{2} m^*$ <sup>9</sup>. Finally, the derivative in Eq. (31) can be written from Eq. (32) as  $\frac{d}{dt} \left( \frac{1}{2} m^* \left( v_B^{|\Phi_5\rangle}(x, t) \right)^2 \right) \approx m^* v_B^{|\Phi_5\rangle}(x, t) \frac{dv_B^{|\Phi_5\rangle}(x, t)}{dt}$ .

Invoking again the negligible role of the quantum potential in this scenario (the spatial derivative of  $Q^{|\Phi_5\rangle}(x, t)$  is negligible in front of the spatial derivative of scalar potential  $A^g = -Ex$ ), one recovers a Newton's law for the Bohmian trajectory  $m^* \frac{dv_B^{|\Phi_5\rangle}(t)}{dt} \approx qE$  to reach again Eq. (31) from a Bohmian perspective.

Finally, we present a summary of the protocol to be followed in a laboratory to obtain the electric field  $E(x, t)$  at a specific time  $t$  and a specific position  $x$  (corresponding to one of the orange points in Fig. 5). For the quantum system described in Eq. (29), the steps are as follows:

- (1) Take an ensemble of identically prepared (pre-selected at time  $t$ ) states  $|\Phi_5(t)\rangle$  and empirically evaluate the weak value  $\mathcal{W}(\hat{V}_x, 0, 0 | |x\rangle, |\Phi_5(t)\rangle)$ .
- (2) From the weak value in step 1), which corresponds to the Bohmian velocity, numerically evaluate the weak value of the kinetic energy as shown in Eq. (32).
- (3) Repeat steps 1) and 2) to empirically evaluate  $\mathcal{W}(\hat{V}_x, 0, t_R | |x\rangle, |\Phi_5(t)\rangle)$  and to numerically compute the corresponding weak value of the kinetic energy at time  $t + t_R$  where  $t_R$  is small (as defined in Section “Finite-difference left-hand derivative (FDLHD)”).
- (4) Numerically evaluate the time derivative of the weak value of the kinetic energy

$$\frac{\partial}{\partial t_R} \text{Re} \left\{ \langle x | \frac{1}{2} m^* \hat{V}_x^2 \hat{U}_{t_R} | \Phi_5(t) \rangle / \langle x | \hat{U}_{t_R} | \Phi_5(t) \rangle \right\}$$

using FDRHD from Eq. (19) and the final numerical outputs obtained in steps 2) and 3).

- (5) Numerically evaluate the electric field  $E(x, t)$  from Eq. (31), using the output in 4) as an input and the  $v_B^{|\Phi_5\rangle}(x, t)$  empirically evaluated in step 1) as the other input.

Notice that the above protocol can be extended further if the empirical weak value of the velocity is replaced by a numerical time derivative of an empirical weak value of the position, as seen in Eq. (27). This possible refined protocol, which involves a second-order time derivative, is demonstrated in the next example.

### Local Lorentz force

We consider a consecutive application of FDLHD in Eq. (18) and FDRHD in Eq. (19), ensuring the gauge invariance of all intermediate expressions, to get:

$$m^* \frac{\partial^2 \mathcal{W}(\hat{X}, t_L, t_R | |x\rangle, |v\rangle)}{\partial t_R \partial t_L} \Bigg|_{\substack{t_R=0 \\ t_L=0}} = q(E(x) + v_B^{(v)} \times B(x)), \tag{33}$$

where  $E(x)$  and  $B(x)$  are the (gauge invariant) electric and magnetic fields at position  $x$  and  $v_B^{(v)}$  is the (gauge invariant) Bohmian velocity of the state  $|v\rangle$  computed from Eq. (25). See Online Appendices L and M.

Notice that the second-order time derivative in Eq. (33) is, in fact, a compact way of referring to a first-order time derivative of another first-order time derivative. The output of the FDLHD given by  $\partial \mathcal{W}(\hat{X}, t_L, t_R | |x\rangle, |v\rangle) / \partial t_L |_{t_L=0} = \mathcal{W}(\hat{V}, 0, t_R | |x\rangle, |v\rangle)$  that satisfies C4 (i.e.,  $[\hat{O}, \hat{F}] = [\hat{X}, \hat{X}] = 0$ ), is used as the input of the FDRHD given by  $\partial \mathcal{W}(\hat{V}, 0, t_R | |x\rangle, |v\rangle) / \partial t_R |_{t_R=0} = \mathcal{W}(\hat{\Xi}, 0, 0 | |x\rangle, |v\rangle)$  that satisfies C5 (i.e.,  $[\hat{O}, \hat{\Lambda}] = [\hat{V}, \hat{V}] = 0$ ), where  $\hat{\Xi} := \frac{i}{\hbar} [\hat{H}, \hat{V}] + \frac{\partial \hat{V}}{\partial t}$  is defined in Online Appendix L. This sequence is precisely what occurs in the Ehrenfest theorem. Two consecutive first-order time derivatives,  $\frac{d}{dt} \langle \psi | \hat{X} | \psi \rangle = \langle \psi | \hat{V} | \psi \rangle$  and  $\frac{d}{dt} \langle \psi | \hat{V} | \psi \rangle = \langle \psi | \hat{\Xi} | \psi \rangle$ , can be compactly written together as  $\frac{d^2}{dt^2} \langle \psi | \hat{X} | \psi \rangle = \langle \psi | \hat{\Xi} | \psi \rangle$ . There are several possible finite-difference approximations to evaluate a mathematical second-order time derivative in Eq. (33). The technical differences among them is not relevant in our discussion<sup>7</sup>. The final result in Eq. (33) is simply a quantum and local version of the (Newton) Lorentz force, which can be used, for example, as a quantum sensor of electromagnetic fields at specific position and time as shown in the numerical example below.

### Numerical example

We consider a quantum system with a magnetic field in the  $z$ -direction, so that  $B = (0, 0, B)$  with  $B = 0.19$  Tesla, and no electric field. To proceed, we need to find a gauge potential  $\mathcal{A}^g$  which obeys  $B = \nabla \times \mathcal{A}^g$ . There is, of course, no unique choice. Here we pick  $\mathcal{A}^g = (0, xB, 0)$  and  $A^g = 0$ . This is called the Landau gauge. In this scenario, the Lorentz force in Eq. (33) is:

$$E(x) + v_B(x) \times B(x) = \{ v_{B,y} B, -v_{B,x} B, 0 \}. \tag{34}$$

The dynamics of the  $z$  direction are not relevant in this scenario, so we assume that an electron moves only in the  $x - y$  plane. Then, the Hamiltonian in Eq. (1) becomes:

$$H = \frac{1}{2m^*} \left( -\hbar^2 \frac{\partial^2}{\partial x^2} + \left( -i\hbar \frac{\partial}{\partial y} - qBx \right)^2 \right). \tag{35}$$

Since this Hamiltonian Eq. (35) has translational invariance in the  $y$  direction, the component of the energy eigenstate in such direction will be a plane wave. On the other hand, it is well-known that the global energy eigenstates of Eq. (35) correspond to those of a displaced harmonic oscillator as described in Online Appendix N.

Since we are interested in initial states that are eigenvalues of the velocity operator, we consider a superposition of 10 energy eigenstates, all with the same  $k_y = 0.0118 \text{ nm}^{-1}$ :

$$\psi_H(x, y, t) = \sum_{n=0}^9 c_{n,k_y}(t) \psi_{n,k_y}(x, y), \tag{36}$$

where the state  $\psi_{n,k_y}(x, y)$  is defined in Eq. (N64) and  $c_{n,k_y}(t)$  in Eq. (N65) in Online Appendix N. By construction, the state  $\psi_H(x, y, t)$  in Eq. (36) is an eigenstate of the velocity in the  $y$ -direction (notice that the

<sup>7</sup>If one uses Eqs. (18) and (19) for the first order time-derivatives, then a simple finite-difference approximation for the second-order time derivative in Eq. (33) is  $(\mathcal{W}_1 - \mathcal{W}_2 - \mathcal{W}_3 + \mathcal{W}_4) / (t_L t_R)$  where  $\mathcal{W}_1 = \mathcal{W}(\hat{y}, 0, t_R | |x\rangle, |v\rangle)$ ,  $\mathcal{W}_2 = \mathcal{W}(\hat{y}, t_L, t_R | |x\rangle, |v\rangle)$ ,  $\mathcal{W}_3 = \mathcal{W}(\hat{y}, 0, 0 | |x\rangle, |v\rangle)$  and  $\mathcal{W}_4 = \mathcal{W}(\hat{y}, t_L, 0 | |x\rangle, |v\rangle)$ . Of course, one can find other finite-difference approximations for the second-order time derivative.

dependence on  $y$  of the term  $\psi_{n,k_y}(x, y)$  is given by the global term  $e^{ik_y y}$  in Eq. (N64) in Online Appendix N, but not in the  $x$  direction. Thus, we focus on the  $y$ -component of Eq. (33) that gives  $-v_{B,x}B$  in Eq. (34), allowing to predict  $B$ .

In Fig. 6, we have plotted the probability distribution of  $|\psi_H(x, y, t)|^2$  at the preparation time ( $t = 0$  ps) and final ( $t = t_f = 20$  ps) times. The evaluation of  $\psi_H(x, y, t)$  at different times is explained in Online Appendix N. We also plot a set of 10 Bohmian trajectories  $x_B(t)$  whose velocity in the  $x$ -component  $v_{B,x}^{|\psi_H\rangle}(x, y, t)$  is computed from the  $x$ -component of the weak value in Eq. (25) as:

$$v_{B,x}^{|\psi_H\rangle} = \text{Re} \left\{ \frac{\langle x, y | \hat{V}_x | \psi_H(t) \rangle}{\langle x, y | \psi_H(t) \rangle} \right\} = \frac{\hbar}{m^*} \text{Im} \left( \frac{\frac{\partial \Psi_H(x, y, t)}{\partial x}}{\Psi_H(x, y, t)} \right), \tag{37}$$

and velocity in the  $y$ -component  $v_{B,y}^{|\psi_H\rangle}(x, y, t)$  is computed from the  $y$ -component of the weak value in Eq. (25) as:

$$v_{B,y}^{|\psi_H\rangle} = \text{Re} \left\{ \frac{\langle x, y | \hat{V}_y | \psi_H(t) \rangle}{\langle x, y | \psi_H(t) \rangle} \right\} = \frac{\hbar}{m^*} \text{Im} \left( \frac{\frac{\partial \Psi_H(x, y, t)}{\partial y}}{\Psi_H(x, y, t)} \right) - \frac{q B x}{m^*}. \tag{38}$$

These weak values of the velocity can be computed in the laboratory from time derivatives of weak values of the positions as in Eq. (27). As discussed for the local work-energy theorem, only one position in configuration space  $\{x, y\}$  and one time  $t$  would have been enough to compute the magnetic field  $B = B(x, y, t)$ . We consider several times and several positions (i.e., the Bohmian trajectories depicted in Fig. 6) to enrich the discussion and to test how robust these predictions are in front of variations of positions and times. The development of Eq. (37) and Eq. (38), plus the computation of the trajectories, is explained in Online Appendix N. Both weak values (velocities) in Eq. (37) and Eq. (38) are plotted in blue in Figs. 7 and 8. Due to the magnetic field and the quantum state  $\psi_H(x, y, t)$ , the Bohmian trajectories show oscillations with a period of 12 ps (corresponding to the mentioned  $\omega = \frac{|q|B}{m^*} = 0.49$  Trad/s define in Online Appendix N) in the  $x$ -direction (as seen in the positive and negative  $x$ -velocities in Fig. 8) and the same oscillation with a net translation in the  $y$ -direction (as seen in the negative  $y$ -velocities in Fig. 7).

In Fig. 7, we have also plotted, in orange, the numerical evaluation of the time derivative of the velocity in Eq. (38). Such a first-order derivative of the velocity corresponds to the second-order derivative of the position of the trajectories plotted in Fig. 6, as indicated in Eq. (27), i.e.,  $\partial \mathcal{W}(\hat{y}, t_L, t_R | x, y, |\psi_H\rangle) / \partial t_L |_{t_L=0} = \mathcal{W}(\hat{V}_y, 0, t_R | x, y, |\psi_H\rangle)$ . Finally, in Fig. 8, we have plotted the predicted value of the magnetic field  $B = B(x, y, t)$  through the  $y$ -component of the Eq. (M48), in Online Appendix M, in the particular case of Eq. (34), giving:

$$B(x, y, t) \approx - \frac{m^*}{q} \frac{\left. \frac{\partial^2 \mathcal{W}(\hat{y}, t_L, t_R | x, y, |\psi_H\rangle)}{\partial t_L \partial t_R} \right|_{t_L=0}}{\left. \frac{\partial \mathcal{W}(\hat{x}, t_L, 0 | x, y, |\psi_H\rangle)}{\partial t_L} \right|_{t_L=0}}, \tag{39}$$

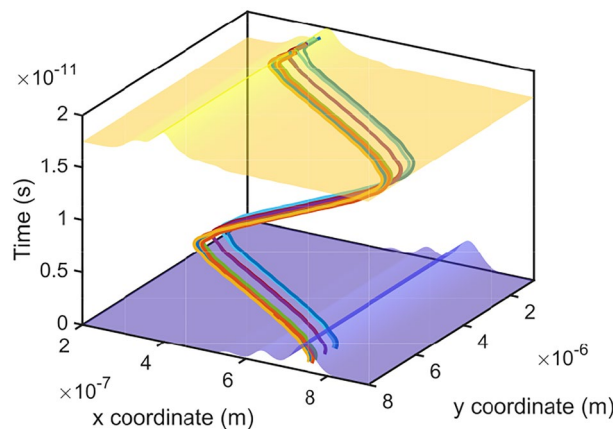


**Fig. 6.** Probability distribution in the  $x - y$  space for the quantum state  $|\psi_H(x, y, t)\rangle^2$  in Eq. (36) at times 0 and 0.2 ps. A set of Bohmian trajectories  $x_B^j(t)$  for  $j = 1, \dots, 10$  are computed by time-integrating the ( $x$ -velocity) weak value in Eq. (37) and the ( $y$ -velocity) weak value in Eq. (38).

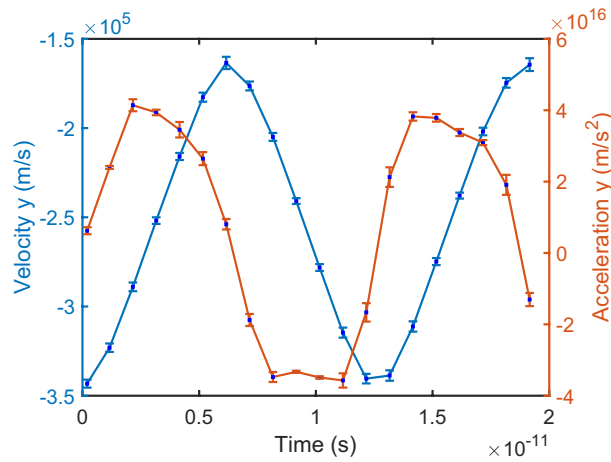


**Fig. 7.** In blue, mean value and standard deviation of the  $y$ -velocity of the 10 trajectories in Fig. 6 at 20 different times (left axis) computed from the weak value in Eq. (38), which also corresponds to the (first order) time derivative of the weak value of the  $y$ -position. In orange, the mean value and standard deviation of the  $y$ -acceleration of the 10 trajectories in Fig. 6 at 20 different times (right axis) computed by the time-derivative of the  $y$ -velocity, which also corresponds to the (second order) time derivative of the weak value of the  $y$ -position.

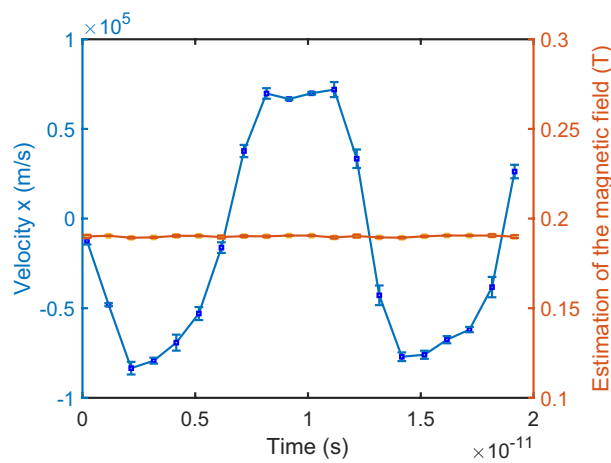


**Fig. 8.** In blue, mean value and standard deviation of the  $x$ -velocity of the 10 trajectories in Fig. 6 at 20 different times (left axis) computed from the weak value in Eq. (37), which corresponds to the (first order) time derivative of the weak value of the post-selected  $x$ -position. In orange, the mean value and standard deviation of the predicted value of the magnetic field computed from the Eq. (39) for the 10 trajectories in Fig. 6. Notice that all values are computed from the weak value of the position post-selected in position and their (first or second-order) time-derivative.

There is an excellent agreement between the magnetic field  $B = 0.19$  Tesla and the value predicted through the time derivative of weak values in Eq. (31). Notice that the last identity in Eq. (39) shows that, in the laboratory, only the weak value of the  $x$ -position, i.e.,  $\mathcal{W}(\hat{x}, t_L, 0 | x, y, |\psi_H\rangle)$ , and  $y$ -position, i.e.,  $\mathcal{W}(\hat{y}, t_L, t_R | x, y, |\psi_H\rangle)$  needs to be evaluated at different times  $t_R$  and  $t_L$ . The result in Eq. (39) can be alternatively justified from a Bohmian perspective, as follows. The first term of the velocity in the  $y$  direction in Eq. (38) can be considered roughly as a constant for a plane wave, i.e.  $\frac{\hbar}{m^*} Im \left( \frac{\partial \Psi_H(x, y, t)}{\partial y} \right) / \Psi_H(x, y, t) = \frac{\hbar k_y}{m^*}$ , where the mentioned quantum potential becomes negligible. Thus, such velocity can be written as  $v_{B,y}^{|\psi_H\rangle}(t) = \hbar k_y / m^* - q B x_B(t) / m^*$  where  $x_B(t)$  is the  $x$ -component of the Bohmian trajectory. Finally, the acceleration (derivative) of this Bohmian velocity in Eq. (38) becomes  $\frac{dv_{B,y}^{|\psi_H\rangle}(x, y, t)}{dt} = -\frac{q B}{m^*} \frac{dx_B(t)}{dt} = -\frac{q B}{m^*} v_{B,x}^{|\psi_H\rangle}(t)$  which is another way of rewriting the expected result in Eq. (39).

Finally, we present a summary of the protocol to be followed in a laboratory to obtain the magnetic field  $B = B(x, y, t)$  at a specific time  $t$  and at specific positions in the a point of the configuration space

$\{x, y\}$  (corresponding to one of the orange points in Fig. 8). For the quantum system described in Eq. (35), the steps are as follows:

- (1) Take an ensemble of identically prepared (pre-selected at  $t$ ) states  $|\psi_H\rangle$  and empirically evaluate the weak value  $\mathcal{W}(\hat{y}, 0, 0|x, |\psi_H\rangle)$ .
- (2) Repeat step 1) to empirically evaluate  $\mathcal{W}(\hat{y}, t_L, 0|x, |\psi_H\rangle)$ ,  $\mathcal{W}(\hat{y}, 0, t_R|x, |\psi_H\rangle)$ , and  $\mathcal{W}(\hat{y}, t_L, t_R|x, |\psi_H\rangle)$  for  $t_L$  and  $t_R$  small enough (as defined in Section “Finite-difference left-hand derivative (FDLHD)”).
- (3) Numerically evaluate the second-order time derivative  $\partial^2 \mathcal{W}(\hat{y}, t_L, t_R|x, y, |\psi_H\rangle) / \partial t_L \partial t_R$  using the four empirical outputs from steps 1) and 2), applying a finite-difference approximation.
- (4) Take an ensemble of identically prepared (pre-selected at  $t$ ) states  $|\psi_H\rangle$  and empirically evaluate the weak value  $\mathcal{W}(\hat{x}, 0, 0|x, |\psi_H\rangle)$ .
- (5) Repeat step 4) to empirically evaluate  $\mathcal{W}(\hat{x}, t_L, 0|x, |\psi_H\rangle)$  for small  $t_L$ .
- (6) Using FDLHD in Eq. (18), numerically evaluate  $\partial \mathcal{W}(\hat{x}, t_L, 0|x, y, |\psi_H\rangle) / \partial t_L$  from the empirical weak values obtained in steps 4) and 5).
- (7) Numerically evaluate the magnetic field  $B(x, y, t)$  from Eq. (39), using as inputs the numerical outputs in steps 3) and 6).

### Which modal theories exhibit time-dependent consistency of weak values?

In the results presented in the previous Section “Examples on the time derivative of weak values”, we have shown that the weak values post-selected in position and its time derivative can be linked to the physical properties of the Bohmian theory. For example, the weak value of the velocity post-selected in position gives the Bohmian velocity of a particle<sup>5</sup>. Thus, it seems that the Bohmian theory is a good framework for predicting weak values post-selected in position and its time derivative. However, Ref.<sup>77</sup> explicitly shows that other Bohm-like theories can be used to predict weak values post-selected in eigenstates other than position eigenstates. The reason why there is an infinite number of Bohm-like theories (also known as modal theories<sup>23</sup>) that can provide a *consistent* picture of quantum phenomena in terms of weak values can be easily evidenced by unraveling the expectation value of the position operator in terms of weak values with an arbitrary post-selected state  $|f\rangle$ . From the identity  $\langle \psi | \hat{X} | \psi \rangle = \langle \psi | \int df |f\rangle \langle f | \hat{X} | \psi \rangle$ , we get:

$$\langle \psi | \hat{X} | \psi \rangle = \int df |\langle \psi | f \rangle|^2 \text{Re} \left\{ \frac{\langle f | \hat{X} | \psi \rangle}{\langle f | \psi \rangle} \right\}. \quad (40)$$

Thus, interpreting the expectation value as a weighted sum of weak values post-selected in  $f$  is *consistent* with Eq. (40). The function  $\text{Re}\{\dots\}$  ensures that the expectation value has no imaginary part. Therefore, each set  $\{|f\rangle\}$  that satisfies  $\int df |f\rangle \langle f| = \mathbb{1}$  can be identified as the primary ontological element of a new Bohm-like theory (i.e., a new  $f$ -modal theory). In particular, the authors of Ref.<sup>77</sup> define the traditional Bohmian theory, where position is the primary ontology, as the x-Bohm theory. Alternatively, they define a p-Bohm theory as a Bohm-like theory where velocity (momentum) is the primary ontological element (i.e., the p-Bohm theory can be used to predict weak values post-selected in velocity eigenstates satisfying Eq. (40)). By comparing the phase-space dynamics offered by the x-Bohm and p-Bohm theories for an arbitrary pre-selected state  $\psi$ , the authors of Ref.<sup>77</sup> conclude that our previous argument that the x-Bohm theory provides a *consistent* explanation of quantum phenomena is quite speculative. Their argument does not negate that the x-Bohm theory provides a *consistent* explanation (i.e., weak values post-selected in position satisfy Eq. (40)), but rather that the x-Bohm theory is merely one *consistent* explanation among an infinite number of possible *consistent*, yet distinct, Bohm-like explanations of quantum phenomena (i.e., weak values post-selected in any eigenstate  $|f\rangle$  that also satisfy Eq. (40)). The summary of the argumentation of Ref.<sup>77</sup> is the following: “When everyone is somebody, then no one’s anybody”.

The developments elaborated in this paper on time derivatives of weak values using LHD and RHD also establish an additional and more restrictive criterion on which post-selected states exhibit also a time-dependent *consistency*. The Ehrenfest theorem deduced from Eq. (9) shows the following time-dependent relationship  $\frac{d}{dt} \langle \psi | \hat{X} | \psi \rangle = \langle \psi | \hat{V} | \psi \rangle$  for any quantum state  $|\psi\rangle$ . Therefore, it seems reasonable to demand a similar *time-dependent consistency* for the weak value that unravels the time derivative of the expectation values. For the position operator, this additional criterion can be written as:

$$\begin{aligned} \frac{d}{dt} \langle \psi | \hat{X} | \psi \rangle &= \langle \psi | \hat{V} | \psi \rangle = \int df |\langle \psi | f \rangle|^2 \text{Re} \left\{ \frac{\langle f | \hat{V} | \psi \rangle}{\langle f | \psi \rangle} \right\} \\ &\stackrel{??}{=} \int df |\langle \psi | f \rangle|^2 \left. \frac{\partial}{\partial t_L} \text{Re} \left\{ \frac{\langle f | \hat{U}_{t_L} \hat{X} | \psi \rangle}{\langle f | \hat{U}_{t_L} | \psi \rangle} \right\} \right|_{t_L=0}. \end{aligned} \quad (41)$$

We have shown in Section “Time Derivative of Weak values” that the accomplishment of the last identity in Eq. (41), which we named *time-dependent consistent* criterion, is not true, in general, for arbitrary post-selected states  $|f\rangle$ . The identity  $\left. \frac{\partial}{\partial t_L} \text{Re} \left\{ \frac{\langle f | \hat{U}_{t_L} \hat{X} | \psi \rangle}{\langle f | \hat{U}_{t_L} | \psi \rangle} \right\} \right|_{t_L=0} = \text{Re} \left\{ \frac{\langle f | \hat{V} | \psi \rangle}{\langle f | \psi \rangle} \right\}$  holds only for very specific post-selected

states  $\langle f|$ . In the particular case of the operator  $\hat{X}$ , from **C4**, we have shown that only the weak values post-selected in position, i.e.,  $|f\rangle = |x\rangle$ , satisfy both Eq. (40) and Eq. (41) for an arbitrary pre-selected state  $|\psi\rangle$ . See Online Appendix O for an alternative demonstration of this result. Thus, the Bohmian theory has a quite privileged status when dealing with weak value post-selected in position and their time derivatives. A similar *time-dependent consistent* criterion can be obtained by replacing the left-hand derivative (LHD) with the right-hand derivative (RHD) in Eq. (41), and ensuring condition **C5**, at the price of fixing the pre-selected state as  $|\psi\rangle = |x\rangle$ .

This previous criterion, on which pre-selected states have *time-dependent consistency*, is an operator-dependent criterion. By replacing the operator  $\hat{X}$  in Eq. (41) by another operator, for example  $\hat{V}$ , other post-selected states are satisfying the *time-dependent consistent* criterion. Again, we notice that there is an infinite set of arbitrarily post-selected states  $|f\rangle$  satisfying:

$$\langle \psi | \hat{V} | \psi \rangle = \int df |\langle \psi | f \rangle|^2 \text{Re} \left\{ \frac{\langle f | \hat{V} | \psi \rangle}{\langle f | \psi \rangle} \right\}. \quad (42)$$

The requirement imposed by the Ehrenfest theorem deduced from Eq. (9) is now  $\frac{d}{dt} \langle \psi | \hat{V} | \psi \rangle = \langle \psi | \hat{\Xi} | \psi \rangle$ , with  $\hat{\Xi} := \frac{i}{\hbar} [\hat{H}, \hat{V}] + \frac{\partial \hat{V}}{\partial t}$  being the operator defined in Online Appendix L. The Ehrenfest theorem can be translated as an additional requirement for the *time-dependent consistency* of the weak values as follows:

$$\begin{aligned} \frac{d}{dt} \langle \psi | \hat{V} | \psi \rangle &= \langle \psi | \hat{\Xi} | \psi \rangle = \int df |\langle \psi | f \rangle|^2 \text{Re} \left\{ \frac{\langle f | \hat{\Xi} | \psi \rangle}{\langle f | \psi \rangle} \right\} \\ &\stackrel{??}{=} \int df |\langle \psi | f \rangle|^2 \left. \frac{d}{dt_L} \text{Re} \left\{ \frac{\langle f | \hat{U}_{t_L} \hat{V} | \psi \rangle}{\langle f | \hat{U}_{t_L} | \psi \rangle} \right\} \right|_{t_L=0}. \end{aligned} \quad (43)$$

In the case of  $\hat{V}$ , from **C4**, we have shown that weak values post-selected in velocity (momentum), i.e.,  $\langle f| = \langle v|$ , satisfy both Eq. (42) and Eq. (43) as they accomplish  $\left. \frac{d}{dt_L} \text{Re} \left\{ \frac{\langle f | \hat{U}_{t_L} \hat{V} | \psi \rangle}{\langle f | \hat{U}_{t_L} | \psi \rangle} \right\} \right|_{t_L=0} = \text{Re} \left\{ \frac{\langle f | \hat{\Xi} | \psi \rangle}{\langle f | \psi \rangle} \right\}$  for arbitrary post-selected states  $|\psi\rangle$ . A similar *time-dependent consistent* criterion can be obtained by changing LHD by RHD in Eq. (43) and ensuring condition **C5**, at the price of fixing the pre-selected state as  $|\psi\rangle = |v\rangle$ .

In principle, it appears that only the first-order time derivative of weak values can be obtained because the post-selected states in Eq. (41) differ from those in Eq. (43). However, by using the equality  $\text{Re} \left\{ \langle v | \hat{V} | x \rangle / \langle v | x \rangle \right\} = \left\{ \text{Re} \langle x | \hat{V} | v \rangle / \langle x | v \rangle \right\}$ , which follows from the hermiticity of  $\hat{V}$ , both Eqs. (41) and (43) can still be satisfied by considering  $|x\rangle$  as the post-selected state and  $|v\rangle$  as the pre-selected state. This is what happens in the numerical results in Section “Local Lorentz force”.

## Conclusions

In physics, the time derivative of a property frequently gives rise to another meaningful property. For example, in classical mechanics, the knowledge of the position allows one to predict the value of the velocity without measuring it, just by taking a first-order time derivative of the position. Even the acceleration of a system (related to the forces acting on the system) can be anticipated from the second-order time derivatives of the position. Since weak values offer empirical insights that cannot be derived from expectation values, this paper investigates what physical insight can be obtained from the time derivative of weak values.

A time derivative of a weak value is not always either a weak value or a gauge-invariant quantity. The necessary and sufficient conditions for the gauge invariance (i.e., empirical observability) of weak values are presented in this paper, i.e., conditions **C1**, **C2** and **C3**. There are weak values in the literature that do not satisfy these conditions, as shown in Table 1 and discussed in Section “Time Derivative of Weak values”. In addition, two more necessary and sufficient conditions (**C4**, **C5**) are presented to ensure that the time derivative of a gauge-invariant weak value also becomes a gauge-invariant weak value. In particular, condition **C4** applies to LHD and condition **C5** to RHD.

We have also discussed how the LHD and RHD can be empirically evaluated in the laboratory through finite-difference approximations of the left- and right-hand time derivatives of weak values, referred to as FDLHD and FDRHD, respectively. We show that FDLHD and FDRHD yield results that are roughly identical to the theoretical LHD and RHD when the latter are gauge invariant.

The time-derivative of weak values can be used, for example, to deduce a local Ehrenfest-like theorem as follows: one weak value (position) measured in the laboratory provides information on two other unmeasured weak values obtained through first-order (velocity) and second-order (acceleration) time derivatives of the first measured weak value. As an example, an electromagnetic field quantum sensor at a local position and time is proposed, utilizing the empirical evaluation of weak values of the position, and computing their time derivatives (through FDLHD and FDRHD).

The findings in this paper reveal an important asymmetry between different post-selected states used to compute weak values. If we want to describe the *local* position, *local* velocity, and *local* acceleration of quantum systems in terms of weak values, and we want these weak values also to satisfy the additional *time-dependent consistency* criteria explained in Eqs. (41) and (43), we conclude that weak values post-selected in position, and somehow also post-selected in velocity, play a quite privileged role—one that cannot be attributed to other weak values post-selected in other quantum states. This privilege, however, implies a limitation on the types of scenarios that are empirically accessible for obtaining simultaneous insight into the local dynamics of quantum

systems through second-order time derivatives of weak values of the position. This second-order time derivative can be used in scenarios pre-selected in velocity eigenstates  $|v\rangle$  and post-selected in position eigenstates  $\langle x|$  (or vice versa). In any case, the second-order time derivative of the weak values involving these wave functions  $\langle x|v(t)\rangle$  is enough to “detect” forces, in general, and electromagnetic fields, in particular.

In this paper, the electric and magnetic fields are treated as external elements of the single-particle Schrödinger equation: the simulated particle used to compute the weak value (which later senses the electromagnetic fields) is affected by these fields, but the fields themselves are not affected by the particle. This approach is the so-called semi-classical treatment of light and matter. The possibility of measuring how electromagnetic fields are distributed in space and time demonstrates the richness of using local-in-position weak values, rather than ensemble values, to characterize physical systems. Future work aims to extend the ideas discussed here to weak values in which both the simulated particle (i.e., matter) and the electromagnetic fields (i.e., light) are quantized<sup>8</sup>.

We emphasize that no fundamental (ontological) conclusions can be drawn from the results of this paper, as all mathematical predictions presented here hold under any interpretation of quantum mechanics. The purpose of this work is not to address the ontological meaning of weak values but rather to investigate their time derivatives and practical applicability. Similarly, the privileged connection between weak values post-selected in position and the Bohmian properties of a quantum system is not intended to argue that Bohmian mechanics is true, but only to highlight its usefulness in envisioning empirical protocols for characterizing novel *local* properties of quantum systems.

### Data availability

The datasets used and/or analysed during the current study are available from the corresponding author on reasonable request.

### Materials availability

Not applicable.

Received: 24 June 2025; Accepted: 10 November 2025

Published online: 26 December 2025

### References

- Aharonov, Y., Albert, D. Z. & Vaidman, L. How the result of a measurement of a component of the spin of a spin-1/2 particle can turn out to be 100. *Phys. Rev. Lett.* **60**, 1351. <https://doi.org/10.1103/PhysRevLett.60.1351> (1988).
- Aharonov, Y. & Vaidman, L. Properties of a quantum system during the time interval between two measurements. *Phys. Rev. A* **41**, 11. <https://doi.org/10.1103/PhysRevA.41.11> (1990).
- Vaidman, L. Weak-measurement elements of reality. *Found. Phys.* **26**, 895. <https://doi.org/10.1007/BF02148832> (1996).
- Aharonov, Y., Bergmann, P. G. & Lebowitz, J. L. Time symmetry in the quantum process of measurement. *Phys. Rev.* **134**, B1410. <https://doi.org/10.1103/PhysRev.134.B1410> (1964).
- Wiseman, H. M. Grounding Bohmian mechanics in weak values and Bayesianism. *New J. Phys.* **9**, 165. <https://doi.org/10.1088/1367-2630/9/6/165> (2007).
- Dürr, D., Goldstein, S. & Zanghì, N. On the weak measurement of velocity in Bohmian mechanics. *J. Stat. Phys.* **134**, 1023. <https://doi.org/10.1007/s10955-008-9674-0> (2009).
- Foo, J. et al. Relativistic Bohmian trajectories of photons via weak measurements. *Nat. Commun.* **13**, 4002. <https://doi.org/10.1038/s41467-022-31608-6> (2022).
- Destefani, C. F. & Oriols, X. Assessing quantum thermalization in physical and configuration spaces via many-body weak values. *Phys. Rev. A* **107**, 012213. <https://doi.org/10.1103/PhysRevA.107.012213> (2023).
- Destefani, C. F. & Oriols, X. Kinetic energy equipartition: A tool to characterize quantum thermalization. *Phys. Rev. Res.* **5**, 033168. <https://doi.org/10.1103/PhysRevResearch.5.033168> (2023).
- Oriols, X., Martín, F. & Sune, J. Implications of the noncrossing property of Bohm trajectories in one-dimensional tunneling configurations. *Phys. Rev. A* **54**, 2594. <https://doi.org/10.1103/PhysRevA.54.2594> (1996).
- Ruseckas, J. & Kaulakys, B. Weak measurement of arrival time. *Phys. Rev. A* **66**, 052106. <https://doi.org/10.1103/PhysRevA.66.052106> (2002).
- Ahnert, S. E. & Payne, M. C. Weak measurement of the arrival times of single photons and pairs of entangled photons. *Phys. Rev. A* **69**, 042103. <https://doi.org/10.1103/PhysRevA.69.042103> (2004).
- Steinberg, A. M. How much time does a tunneling particle spend in the barrier region?. *Phys. Rev. Lett.* **74**, 2405. <https://doi.org/10.1103/PhysRevLett.74.2405> (1995).
- Campo, D. & Parentani, R. Space-time correlations in inflationary spectra: A wave-packet analysis. *Phys. Rev. D* **70**, 105020. <https://doi.org/10.1103/PhysRevD.70.105020> (2004).
- Kofman, A. G., Ashhab, S. & Nori, F. Nonperturbative theory of weak pre- and post-selected measurements. *Phys. Rep.* **520**(2), 43. <https://doi.org/10.1016/j.physrep.2012.07.001> (2012).
- Adam, P. & Diosi, L. Sequential unsharp measurement of photon polarization. *Phys. Rev. A* **107**(6), 063706. <https://doi.org/10.1103/PhysRevA.107.063706> (2023).
- Brout, R., Massar, S., Parentani, R. & Spindel, P. A primer for black hole quantum physics. *Phys. Rep.* **260**, 329. [https://doi.org/10.1016/0370-1573\(95\)00008-5](https://doi.org/10.1016/0370-1573(95)00008-5) (1995).
- Brun, T., Diosi, L. & Strunz, W. T. Test of weak measurement on a two- or three-level system. *Phys. Rev. A* **77**, 032101. <https://doi.org/10.1103/PhysRevA.77.032101> (2008).

<sup>8</sup>For example, in the framework of cavity quantum electrodynamics Ref.53, where light is confined within an optical resonator, if we assume that energy restrictions ensure that only the fundamental mode of the resonator is available, the quantum treatment of light can be readily incorporated into the Schrödinger equation used in this work. This essentially requires adding the pair of non-commuting operators that arise from the canonical quantization of the classical canonical degrees of freedom, i.e., the Fourier amplitude of the single mode, to describe the quantum light inside the optical cavity Ref.78

19. Botero, A. & Reznik, B. Quantum-communication protocol with correlated weak measurements. *Phys. Rev. A* **61**, 050301(R). <https://doi.org/10.1103/PhysRevA.61.050301> (2000).
20. Hofmann, H. F. Complete characterization of post-selected quantum statistics using weak measurement tomography. *Phys. Rev. A* **81**, 012103. <https://doi.org/10.1103/PhysRevA.81.012103> (2010).
21. Kastner, R. E. Weak values and consistent histories in quantum theory. *Stud. Hist. Philos. M P* **35**, 57. <https://doi.org/10.1016/j.shpsb.2003.02.001> (2004).
22. Leavens, C. R. Weak measurements from the point of view of Bohmian mechanics. *Found. Phys.* **35**, 469. <https://doi.org/10.1007/s10701-004-1984-8> (2005).
23. Pandey, D., Sampaio, R., Ala-Nissila, T., Albareda, G. & Oriols, X. Identifying weak values with intrinsic dynamical properties in modal theories. *Phys. Rev. A* **103**, 052219. <https://doi.org/10.1103/PhysRevA.103.052219> (2021).
24. Agarwal, G. S. & Pathak, P. K. Realization of quantum-mechanical weak values of observables using entangled photons. *Phys. Rev. A* **75**, 032108. <https://doi.org/10.1103/PhysRevA.75.032108> (2007).
25. Marian, D., Zanghi, N. & Oriols, X. Weak values from displacement currents in multiterminal electron devices. *Phys. Rev. Lett.* **116**, 110404. <https://doi.org/10.1103/PhysRevLett.116.110404> (2016).
26. Subramanian, M., Mathew, A. & Muralidharan, B. Resonant weak-value enhancement for solid-state quantum metrology. *Phys. Rev. Appl.* **20**, 044065. <https://doi.org/10.1103/PhysRevApplied.20.044065> (2023).
27. Pryde, G. J., O'Brien, J. L., White, A. G., Ralph, T. C. & Wiseman, H. M. Measurement of quantum weak values of photon polarization. *Phys. Rev. Lett.* **94**, 220405. <https://doi.org/10.1103/PhysRevLett.94.220405> (2005).
28. Jordan, A. N. & Korotkov, A. N. Uncollapsing the wavefunction by undoing quantum measurements. *Contemp. Phys.* **51**, 125. <https://doi.org/10.1080/00107510903385292> (2010).
29. Jordan, A. N., Trauzettel, B. & Burkard, G. Weak-measurement theory of quantum-dot spin qubits. *Phys. Rev. B* **76**, 155324. <https://doi.org/10.1103/PhysRevB.76.155324> (2007).
30. Korotkov, A. N. & Jordan, A. N. Undoing a weak quantum measurement of a solid-state qubit. *Phys. Rev. Lett.* **97**, 166805. <https://doi.org/10.1103/PhysRevLett.97.166805> (2006).
31. Romito, A., Gefen, Y. & Blanter, Y. M. Weak values of electron spin in a double quantum dot. *Phys. Rev. Lett.* **100**, 056801. <https://doi.org/10.1103/PhysRevLett.100.056801> (2008).
32. Zilberberg, O., Romito, A. & Gefen, Y. Null values and quantum state discrimination. *Phys. Rev. Lett.* **106**, 080405. <https://doi.org/10.1103/PhysRevLett.106.080405> (2011).
33. Hariri, A., Curic, D., Giner, L. & Lundeen, J. S. Experimental realization of weak value amplification using a single photon source. *Phys. Rev. A* **100**, 032119. <https://doi.org/10.1103/PhysRevA.100.032119> (2019).
34. Ramos, R., Spierings, D., Racicot, I. & Steinberg, A. M. Measurement of the time spent by a tunneling atom within the barrier region. *Nature* **583**, 529. <https://doi.org/10.1038/s41586-020-2490-7> (2020).
35. Dressel, J., Malik, M., Miatto, F. M., Jordan, A. N. & Boyd, R. W. Colloquium: Understanding quantum weak values: Basics and applications. *Rev. Mod. Phys.* **86**, 307. <https://doi.org/10.1103/RevModPhys.86.307> (2014).
36. Lundeen, J. S., Sutherland, B., Patel, A., Stewart, C. & Bamber, C. Direct measurement of the quantum wavefunction. *Nature* **474**(7350), 188. <https://doi.org/10.1038/nature10120> (2011).
37. Zhu, J. et al. Reconstructing the wave function through the momentum weak value. *Phys. Rev. A* **104**(3), 032221. <https://doi.org/10.1103/PhysRevA.104.032221> (2021).
38. Ritchie, N. W. M., Story, J. G. & Hulet, R. G. Realization of a measurement of a 'weak value'. *Phys. Rev. Lett.* **66**(9), 1107. <https://doi.org/10.1103/PhysRevLett.66.1107> (1991).
39. Resch, K. J., Lundeen, J. S. & Steinberg, A. M. Experimental realization of the quantum box problem. *Phys. Lett. A* **324**, 125. <https://doi.org/10.1016/j.physleta.2004.02.042> (2004).
40. Williams, N. S. & Jordan, A. N. Weak values and the Leggett-Garg inequality in solid-state qubits. *Phys. Rev. Lett.* **100**, 026804. <https://doi.org/10.1103/PhysRevLett.100.026804> (2008).
41. Brunner, N., Scarani, V., Wegmuller, M., Legré, M. & Gisin, N. Direct measurement of superluminal group velocity and signal velocity in an optical fiber. *Phys. Rev. Lett.* **93**, 203902. <https://doi.org/10.1103/PhysRevLett.93.203902> (2004).
42. Kocsis, S. et al. Observing the average trajectories of single photons in a two-slit interferometer. *Science* **332**, 1170. <https://doi.org/10.1126/science.1202218> (2011).
43. Hosten, O. & Kwiat, P. Observation of the spin Hall effect of light via weak measurements. *Science* **319**, 787. <https://doi.org/10.1126/science.1152697> (2008).
44. Starling, D. J., Dixon, P. B., Jordan, A. N. & Howell, J. C. Optimizing the signal-to-noise ratio of a beam-deflection measurement with interferometric weak values. *Phys. Rev. A* **80**, 041803(R). <https://doi.org/10.1103/PhysRevA.80.041803> (2009).
45. Starling, D. J., Dixon, P. B., Jordan, A. N. & Howell, J. C. Precision frequency measurements with interferometric weak values. *Phys. Rev. A* **82**, 063822. <https://doi.org/10.1103/PhysRevA.82.063822> (2010).
46. Braverman, B. & Simon, C. Proposal to observe the nonlocality of Bohmian trajectories with entangled photons. *Phys. Rev. Lett.* **110**, 060406. <https://doi.org/10.1103/PhysRevLett.110.060406> (2013).
47. Healey, R. *Gauging What's Real: The Conceptual Foundations of Contemporary Gauge Theories* (Oxford University Press, Oxford, 2007).
48. Kobe, D. H. & Wen, E. T. Gauge invariance in quantum mechanics: Charged harmonic oscillator in an electromagnetic field. *J. Phys. A: Math. Gen.* **15**(3), 787. <https://doi.org/10.1088/0305-4470/15/3/018> (1982).
49. Stokes, A. & Nazir, A. Identification of Poincaré-gauge and multipolar nonrelativistic theories of QED. *Phys. Rev. A* **104**(3), 032227. <https://doi.org/10.1103/PhysRevA.104.032227> (2021).
50. Jackson, J. D. & Okun, L. B. Historical roots of gauge invariance. *Rev. Mod. Phys.* **73**(3), 663. <https://doi.org/10.1103/RevModPhys.73.663> (2001).
51. Cohen-Tannoudji, C., Diu, B. & Laloe, F. *Quantum Mechanics* Vol. 1 (Wiley, New York, 1986).
52. Aharonov, Y. & Bohm, D. Significance of electromagnetic potentials in the quantum theory. *Phys. Rev.* **115**(3), 485. <https://doi.org/10.1103/PhysRev.115.485> (1959).
53. Grynberg, G., Aspect, A. & Fabre, C. *Introduction to Quantum Optics: From the Semi-classical Approach to Quantized Light* (Cambridge University Press, New York, 2010).
54. Ballentine, L. E. *Quantum Mechanics: A Modern Development* (World Scientific Publishing Company, Singapore, 2000).
55. Sokolovski, D. Weak measurements measure probability amplitudes (and very little else). *Phys. Lett. A* **380**(18–19), 1593. <https://doi.org/10.1016/j.physleta.2016.02.051> (2016).
56. Matzkin, A. Weak values and quantum properties. *Found. Phys.* **49**(3), 298. <https://doi.org/10.1007/s10701-019-00245-3> (2019).
57. Reznik, B. & Aharonov, Y. Time-symmetric formulation of quantum mechanics. *Phys. Rev. A* **52**, 2538. <https://doi.org/10.1103/PhysRevA.52.2538> (1995).
58. Hiley, B. J. Weak values: Approach through the Clifford and Moyal algebras. *J. Phys. Conf. Ser.* **361**, 012014. <https://doi.org/10.1088/1742-6596/361/1/012014> (2012).
59. Kastner, R. E. Demystifying weak measurements. *Found. Phys.* **47**, 697. <https://doi.org/10.1007/s10701-017-0085-4> (2017).
60. Cohen, E. What weak measurements and weak values really mean: Reply to Kastner. *Found. Phys.* **47**(10), 1261. <https://doi.org/10.1007/s10701-017-0107-2> (2017).
61. Sinclair, J., Spierings, D., Brodutch, A. & Steinberg, A. M. Interpreting weak value amplification with a toy realist model. *Phys. Lett. A* **383**(24), 2839. <https://doi.org/10.1016/j.physleta.2019.06.010> (2019).

62. Garretson, J. L., Wiseman, H. M., Pope, D. T. & Pegg, D. T. The uncertainty relation in ‘which-way’ experiments: How to observe directly the momentum transfer using weak values. *J. Opt. B: Quantum Semiclass Opt.* **6**, S506. <https://doi.org/10.1088/1464-4266/6/6/008> (2004).
63. Rebufello, E. et al. Anomalous weak values via a single photon detection. *Light Sci. Appl.* **10**, 106. <https://doi.org/10.1038/s41377-021-00539-0> (2021).
64. Cohen, E. & Pollak, E. Determination of weak values of quantum operators using only strong measurements. *Phys. Rev. A* **98**, 042112. <https://doi.org/10.1103/PhysRevA.98.042112> (2018).
65. Berche, B., Malterre, D. & Medina, E. Gauge transformations and conserved quantities in classical and quantum mechanics. *Am. J. Phys.* **84**(8), 616. <https://doi.org/10.1119/1.4955153> (2016).
66. Tumulka, R. Limitations to genuine measurements in ontological models of quantum mechanics. *Found. Phys.* **52**(5), 110. <https://doi.org/10.1007/s10701-022-00633-2> (2022).
67. Kobe, D. H. & Yang, K. H. Gauge transformation of the time-evolution operator. *Phys. Rev. A* **32**(2), 952. <https://doi.org/10.1103/PhysRevA.32.952> (1985).
68. Svensson, B. E. Y. Pedagogical review of quantum measurement theory with an emphasis on weak measurements. *Quanta* **2**, 18. <https://doi.org/10.12743/quanta.v2i1.12> (2013).
69. Wiseman, H. & Milburn, G. J. *Quantum Measurement and Control* (Cambridge University Press, New York, 2009).
70. Ehrenfest, P. Bemerkung über die angenäherte Gültigkeit der klassischen Mechanik innerhalb der Quantenmechanik. *Z. Angew. Phys.* **45**, 455. <https://doi.org/10.1007/BF01329203> (1927).
71. Dressel, J. & Jordan, A. N. Significance of the imaginary part of the weak value. *Phys. Rev. A* **85**, 012107. <https://doi.org/10.1103/PhysRevA.85.012107> (2012).
72. Jozsa, R. Complex weak values in quantum measurement. *Phys. Rev. A* **76**(4), 044103. <https://doi.org/10.1103/PhysRevA.76.044103> (2007).
73. Freericks, J. K. How to measure the momentum of single quanta. arXiv. (2023). <https://doi.org/10.48550/arXiv.2302.12303>.
74. Deotto, E. & Ghirardi, G. C. Bohmian mechanics revisited. *Found. Phys.* **28**, 1. <https://doi.org/10.1023/A:101875202576> (1998).
75. Nelson, E. Derivation of the Schrödinger equation from Newtonian mechanics. *Phys. Rev.* **150**, 1079. <https://doi.org/10.1103/PhysRev.150.1079> (1966).
76. Bohm, D. & Hiley, B. J. Non-locality and locality in the stochastic interpretation of quantum mechanics. *Phys. Rep.* **172**, 93. [https://doi.org/10.1016/0370-1573\(89\)90160-9](https://doi.org/10.1016/0370-1573(89)90160-9) (1989).
77. Pang, A. O. et al. Experimental comparison of Bohm-like theories with different guidance equations. *Quantum* **4**, 365. <https://doi.org/10.22331/q-2020-11-26-365> (2020).
78. Destefani, C. F., Villani, M., Cartoixa, X., Feiginov, M. & Oriols, X. Resonant tunneling diodes in semiconductor microcavities: Modeling polaritonic features in the THz displacement current. *Phys. Rev. B* **106**, 205306. <https://doi.org/10.1103/PhysRevB.106.205306> (2022).

## Acknowledgements

The work has benefited from discussions with Xabier Oianguren-Asua.

## Author contributions

Not applicable.

## Funding

This research was funded by Spain’s Ministerio de Ciencia, Innovación y Universidades under Grants PID2021-127840NB-I00 (MICINN/AEI/FEDER, UE), PDC2023-145807-I00 (MICINN/AEI/FEDER, UE) and PID2024-161603NB-I00 (MICINN/AEI/FEDER, UE), and European Union’s Horizon 2020 research and innovation program DigiQ under grant proposal ID:101084035

## Declarations

## Competing interests

The author declares that he has no competing interest.

## Additional information

**Supplementary Information** The online version contains supplementary material available at <https://doi.org/10.1038/s41598-025-28260-7>.

**Correspondence** and requests for materials should be addressed to X.O.

**Reprints and permissions information** is available at [www.nature.com/reprints](http://www.nature.com/reprints).

**Publisher’s note** Springer Nature remains neutral with regard to jurisdictional claims in published maps and institutional affiliations.

**Open Access** This article is licensed under a Creative Commons Attribution-NonCommercial-NoDerivatives 4.0 International License, which permits any non-commercial use, sharing, distribution and reproduction in any medium or format, as long as you give appropriate credit to the original author(s) and the source, provide a link to the Creative Commons licence, and indicate if you modified the licensed material. You do not have permission under this licence to share adapted material derived from this article or parts of it. The images or other third party material in this article are included in the article’s Creative Commons licence, unless indicated otherwise in a credit line to the material. If material is not included in the article’s Creative Commons licence and your intended use is not permitted by statutory regulation or exceeds the permitted use, you will need to obtain permission directly from the copyright holder. To view a copy of this licence, visit <http://creativecommons.org/licenses/by-nc-nd/4.0/>.

© The Author(s) 2025